Synthesis, DNA-binding ability and anticancer activity of benzothiazole/benzoxazole-pyrrolo[2,1-c][1,4]benzodiazepine conjugates

ARTICLE *in* BIOORGANIC & MEDICINAL CHEMISTRY · JULY 2010

Impact Factor: 2.79 · DOI: 10.1016/j.bmc.2010.05.007 · Source: PubMed

13 AUTHORS, INCLUDING:

Ahmed Kamal
Indian Institute of Chemical Technology
489 PUBLICATIONS **6,086** CITATIONS
SEE PROFILE

Janaki Ramaiah
Indian Institute of Chemical Technology
61 PUBLICATIONS **647** CITATIONS
SEE PROFILE

G Narahari Sastry
Indian Institute of Chemical Technology
262 PUBLICATIONS **5,153** CITATIONS
SEE PROFILE

Aarti Juvekar
Advanced Centre for Treatment, Research …
29 PUBLICATIONS **482** CITATIONS
SEE PROFILE

Bioorganic & Medicinal Chemistry 18 (2010) 4747–4761

Contents lists available at ScienceDirect

Bioorganic & Medicinal Chemistry

journal homepage: www.elsevier.com/locate/bmc

Synthesis, DNA-binding ability and anticancer activity of benzothiazole/benzoxazole–pyrrolo[2,1-*c*][1,4]benzodiazepine conjugates

Ahmed Kamal [a,*], K. Srinivasa Reddy [a], M. Naseer A. Khan [a], Rajesh V. C. R. N. C. Shetti [a], M. Janaki Ramaiah [a], S. N. C. V. L. Pushpavalli [a], Chatla Srinivas [a], Manika Pal-Bhadra [a], Mukesh Chourasia [b], G. Narahari Sastry [b], Aarti Juvekar [c], Surekha Zingde [c], Madan Barkume [c]

[a] *Chemical Biology Laboratory, Division of Organic Chemistry, Indian Institute of Chemical Technology, Hyderabad 500 607, India*
[b] *Molecular Modeling Group, Division of Organic Chemistry, Indian Institute of Chemical Technology, Hyderabad 500 607, India*
[c] *Advanced Centre for Treatment, Research and Education in Cancer (ACTREC), Navi Mumbai 410 208, India*

ARTICLE INFO

Article history:
Received 23 March 2010
Revised 1 May 2010
Accepted 4 May 2010
Available online 7 May 2010

Keywords:
Pyrrolobenzodiazepine
Benzothiazole
Benzoxazole, DNA-binding affinity
Anticancer activity
Molecular modelling
In vivo efficacy

ABSTRACT

A series of benzothiazole and benzoxazole linked pyrrolobenzodiazepine conjugates attached through different alkane or alkylamide spacers was prepared. Their anticancer activity, DNA thermal denaturation studies, restriction endonuclease digestion assay and flow cytometric analysis in human melanoma cell line (A375) were investigated. One of the compounds of the series **17d** showed significant anticancer activity with promising DNA-binding ability and apoptosis caused G0/G1 phase arrest at sub-micromolar concentrations. To ascertain the binding mode and understand the structural requirement of DNA binding interaction, molecular docking studies using GOLD program and more rigorous 2 ns molecular dynamic simulations using Molecular Mechanics-Poisson–Boltzman Surface Area (MM-PBSA) approach including the explicit solvent were carried out. Further, the compound **17d** was evaluated for in vivo efficacy studies in human colon cancer HT29 xenograft mice.

1. Introduction

DNA has been considered for a long time as a favoured target for cancer chemotherapeutic agents. On the other hand, achievement of the desired sequence selectivity with DNA-binding agents is considered to be one of the most difficult tasks. Meanwhile, for the past few years certain molecules are being developed and one such class are naturally occurring pyrrolo[2,1-*c*][1,4]benzodiazepines. These tricyclic molecules have been isolated from various *Streptomyces* species and typical examples of which include DC-81, anthramycin, tomaymycin, sibiromycin and neothramycins.[1] From a mechanistic point of view, these molecules exert their biological activity by covalently binding to NH_2 of guanine in the minor groove of DNA through the imine or imine equivalent functionality at N10–C11 position of the PBD ring system.[2] Moreover, the PBDs bind to DNA sequence selectively and have potential not only as antitumour agents but also as gene regulators and probes of DNA structure.[3] The excellent antitumour potential of these molecules has stimulated the synthesis of a large number of hybrids and dimers.[4] Some of these analogues have shown significant DNA-binding ability with promising anticancer activity. One of the analogues, SJG-136 is under clinical evaluation.[5]

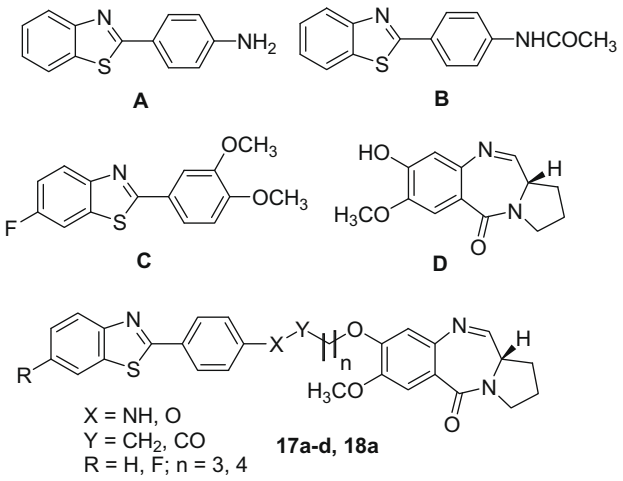

Figure 1. Chemical structures of anticancer active molecules.

* Corresponding author. Tel.: +91 40 27193157; fax: +91 40 27193189.
E-mail address: ahmedkamal@iict.res.in (A. Kamal).

0968-0896/$ - see front matter © 2010 Elsevier Ltd. All rights reserved.
doi:10.1016/j.bmc.2010.05.007

Benzothiazoles demonstrated interesting pharmacological activities and in the past two decades they have been extensively studied for their anticancer activity.[6] 2-(4-Aminophenyl)benzothiazoles[7] and their corresponding N-acetylated derivatives (Fig. 1A and B)[8] have showed surprisingly remarkable anticancer activity against certain cancer cell lines particularly against breast, colon and ovarian cell lines in in vitro anticancer screening program of the National Cancer Institute (NCI). The anticancer activity of these molecules is assumed to be due to the formation of reactive intermediates that can bind covalently to DNA.[9] Some other related class of benzothiazoles have also shown good antitumour activity.[10] Surprisingly, among an extended library of very close structural analogues, only a compound possessing a 2-(3,4-dimethoxyphenyl) group and a fluoro substituent in the benzothiazole ring, especially at the 5-position exhibited potent anticancer activity (Fig. 1C). However, compounds with no substituent in the benzothiazole moiety retained sub-micromolar activity against certain cancer cell lines. The definitive molecular target responsible for the antitumour activity of this series has not been identified and mechanistically, this new series of agents contrasts with the 2-(4-aminophenyl)benzothiazoles. Similarly, isosteric benzoxazoles have also demonstrated good anticancer activity.[11]

In continuation of our previous studies[12] on the structural modifications of pyrrolo[2,1-*c*][1,4]benzodiazepines and encouraging antitumour activity of benzothiazole as well as isosteric benzoxazoles we herein wish to report the synthesis, DNA-binding ability, molecular modelling, anticancer activity and in vivo efficacy study of C8-coupled benzothiazole/benzoxazole–PBD conjugates. In order to identify agents with better potency, systematic structural modifications were made with different alkoxyamide and alkane spacers.

2. Chemistry

The synthesis of benzoxazole intermediates **3a**,**b** was carried out by the condensation of 2-aminophenol with 4-benzyloxybenzaldehyde precursors to provide **1a**,**b**. Compounds **1a**,**b** were converted to **2a**,**b** by oxidative cyclization, which were then subjected to debenzylation to afford **3a**,**b** (Scheme 1). The other key intermediates **4a**,**b** were obtained by the condensation of 2-aminothiophenol with substituted benzaldehydes as previously reported.[10,13] The benzothiazole/benzoxazole bromoalkyl spacers were prepared by treating hydroxyl benzoxazoles/benzothiazole (**3a**,**b** and **4a**,**b**) with dibromo alkanes by potassium carbonate in acetone reflux affords the desired bromoalkoxy benzothiazole/benzoxazoles (**5a**–**f**, Scheme 2). The bromoamide derivatives of benzothiazoles (**9a**–**c**) were prepared according to Scheme 3. The synthesis of precursors **9a**–**c** was carried out by Jacobson's cyclization approach. The treatment of 4-fluoroaniline/aniline with 4-nitrobenzoyl chloride in pyridine gave **6a**,**b**. These compounds were further converted to its corresponding thio-derivative **7a**,**b** using Lawesson's reagent by refluxing in toluene. Finally, the compounds **7a**,**b** were cyclized by potassium ferricyanide according to Jacobson's method[14,7b] and were reduced to their amino precursors (**8a**,**b**). These were coupled to the bromopentanoyl chloride resulting to produce **9a**–**c** (Scheme 3). The synthesis of the desired benzothiazole/benzoxazole–pyrrolo[2,1-*c*][1,4] benzodiazepine hybrids (**17a**–**f**, **18a**,**b**) was carried out by the synthetic sequence illustrated in Schemes 4 and 5. The synthesis of the starting material 2-nitrobenzoic acid (**10**) was prepared by employing the commercially available vanillin. Oxidation of vanillin, nitration, followed by benzylation as reported in the literature[15] provided 2-nitrobenzoic acid (**10**). This was further coupled with L-proline methyl ester hydrochloride to afford the nitro ester derivative (**11**). The ester group of this compound was then reduced with DIBAL-H to produce the corresponding aldehyde derivative **12**, which upon protection with EtSH/TMSCl yielded **13**. Compound **13** upon debenzylation afforded (2*S*)-*N*-(4-hydroxy-5-methoxy-2-nitrobenzoyl) pyrrolidine-2-carboxaldehyde diethylthioacetal (**14**), nitrothioacetal intermediates upon reduction with $SnCl_2{\cdot}2H_2O$ in refluxing methanol gave the aminothioacetal precursors (**15**). This upon thiol deprotection by $HgCl_2/CaCO_3$ in CH_3CN–H_2O at room temperature afforded the required DC-81 (**16**). This intermediate was treated with 2-[4-(*n*-alkyloxy)-phenyl) benzothiazoles (**5a**–**d**) or 2-[4-(*n*-alkyloxy)-phenyl) benzoxazoles (**5e**,**f**) or bromoalkoxyamido benzothiazoles (**5e**,**f**) by employing KI/K_2CO_3 in acetone at room temperature to afford the required PBD conjugates **17a**–**f** and **18a**,**b** (Schemes 4 and 5). However, when bromobutyrylamide of benzothiazole (**9c**) was coupled with the PBD precursor (**16**) the expected product **18c** was not obtained and instead benzothaizole derivative was cyclized to the corresponding pyrrolidinone derivative **19** (Scheme 6).[16]

3. Results and discussion

3.1. Thermal denaturation studies

The DNA binding activity for these new C8-linked benzoxazole or benzothiazole–PBD conjugates (**17a**–**f**, **18a**,**b**) was examined by thermal denaturation studies using calf thymus (CT) DNA.[17] Melting studies showed that these compounds stabilize the thermal helix→coil or melting stabilization (ΔT_m) for the CT-DNA duplex at pH 7.0, incubated at 37 °C, where PBD/DNA molar ratio is 1:5. The data for the compounds **17a**–**f**, **18a**,**b** is included in Table 1 along with naturally occurring DC-81. It is observed that some of the prepared compounds have shown good DNA binding property compared to naturally occurring PBD-like DC-81. It is also observed that benzothiazole–PBD conjugates with five-carbon spacer (**17c**,**d**) exhibited better DNA-binding affinity than their corresponding four-carbon spacer benzothiazole–PBD conjugates (**17a**,**b**). The amide conjugates (**18a**,**b**) show less binding affinity than their counter part ether derivatives (**17c**,**d**). The substitution of fluorine atom on benzothiazole moiety of **18a** elevates the DNA melting temperature considerably. Another observation is that the replacement of sulfur atom with oxygen does not alter the binding ability.

3.2. Restriction endonuclease digestion assay

The restriction endonuclease inhibition studies (RED assay) were carried out to further confirm the binding ability of these

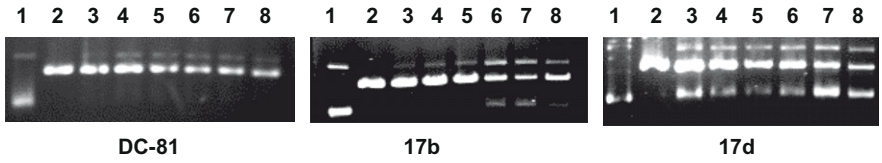

Figure 2. Restriction endonuclease digestion assay (RED_{100}-assay) for *A*-C8-linked PBD with CT-DNA inhibitory activity of DC-81, **17b** and **17d** on the cleavage of plasmid pBR322 by restriction endonuclease *Bam*H1 (20 units in 2 μL) for 1 h at 37 °C. The products were separated by agarose gel electrophoresis and visualized by ethidium bromide staining under UV illumination. Lane 1: control pBR322; lane 2: complete digest of pBR322 by *Bam*H1; lanes 3–8: increasing concentration of DC-81, **17b** and **17d** ranging from 5, 10, 15, 20, 25 and 30 μM.

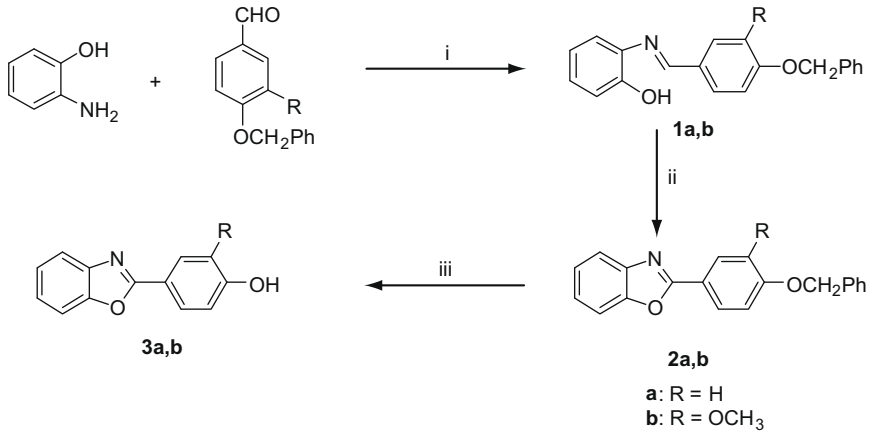

Scheme 1. Reagents and conditions: (i) ethanol, reflux, 1 h; (ii) $Pb(OAc)_4$, $CHCl_3$, reflux, 1 h, (iii) Pd/C, H_2, ethyl acetate, rt, 30 min.

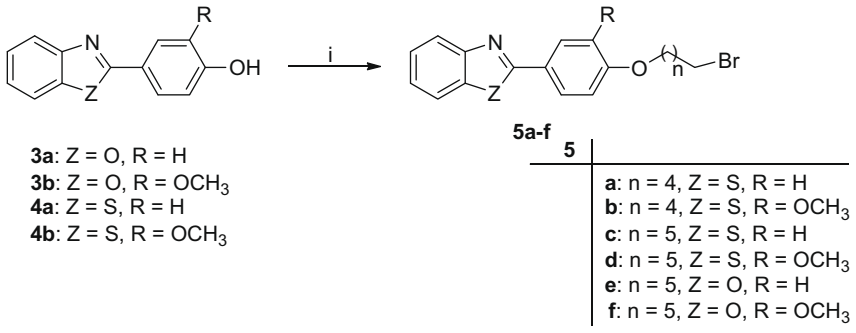

Scheme 2. Reagents and conditions: (i) dibromoalkanes, K_2CO_3, acetone, 24 h, reflux.

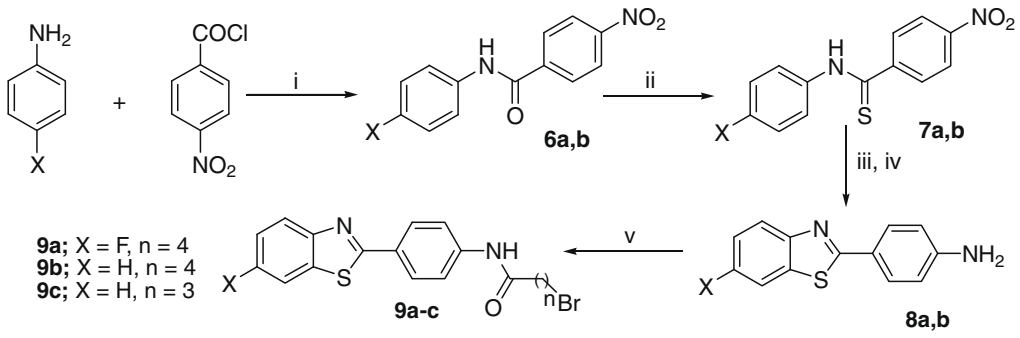

Scheme 3. Reagents and conditions: (i) pyridine, reflux, 1 h; (ii) Lawesson's reagent, HMPA, 100 °C, 5 h; (iii) $K_3Fe(CN)_6$, aq NaOH, 90 °C, (iv) $SnCl_2{\cdot}2H_2O$, methanol, reflux, 5 h; (v) *n*-alkylbromoacid chloride, Et_3N, THF, 0 °C to rt, 30 min.

PBD conjugates to DNA particularly at G-rich sites. The experimental protocol described in the previous studies has been employed.[18] The dose dependent inhibition (0–30 μM) of the compounds with DNA cleavage activity of *Bam*H1 was studied using pBR 322 vector DNA. The results of this experiment clearly showed that **17d** is the most effective DNA binding compound among all the compounds tested in this series. The order of binding to DNA is **17d** > **17b** > DC-81 and also dose dependent inhibition of *Bam*H1 was observed with these PBD conjugates.

3.2.1. Molecular modelling studies

The variations in the DNA-binding affinities with respect to linker length and substitution of sulfur, oxygen and methoxy in this class of molecules were investigated by molecular modelling approaches employing docking[19] and molecular dynamic studies.[21] About eight different DNA sequences were examined to investigate the most suitable DNA sequence for carrying out the docking studies. Among these, sequence A (5′-CGCAGAAATTTCTGCG-3′) provides the best correlation with the experimental results which may be traced to the possession of optimal AT rich region in this model strand. Molecular Mechanics-Poisson–Boltzman Surface Area (MM-PBSA) approach of AMBER molecular dynamics (MD) package was used to investigate the free binding energies ($\Delta G_{bind,solv}$) of the DNA–ligand complex.[20]

A quick analysis of the docking results reveals that the binding affinities of DNA–ligand complexes have dependence on the linker length (Table 2 and Fig. 3). Compound **17d** has showed the highest docking score of 73.04. The linker of heterodimers localized in the span of six AT sites (5′-CGC*AGAAATTT*CTGCG-3′) are observed in each DNA–ligand complex. The final docked conformation of

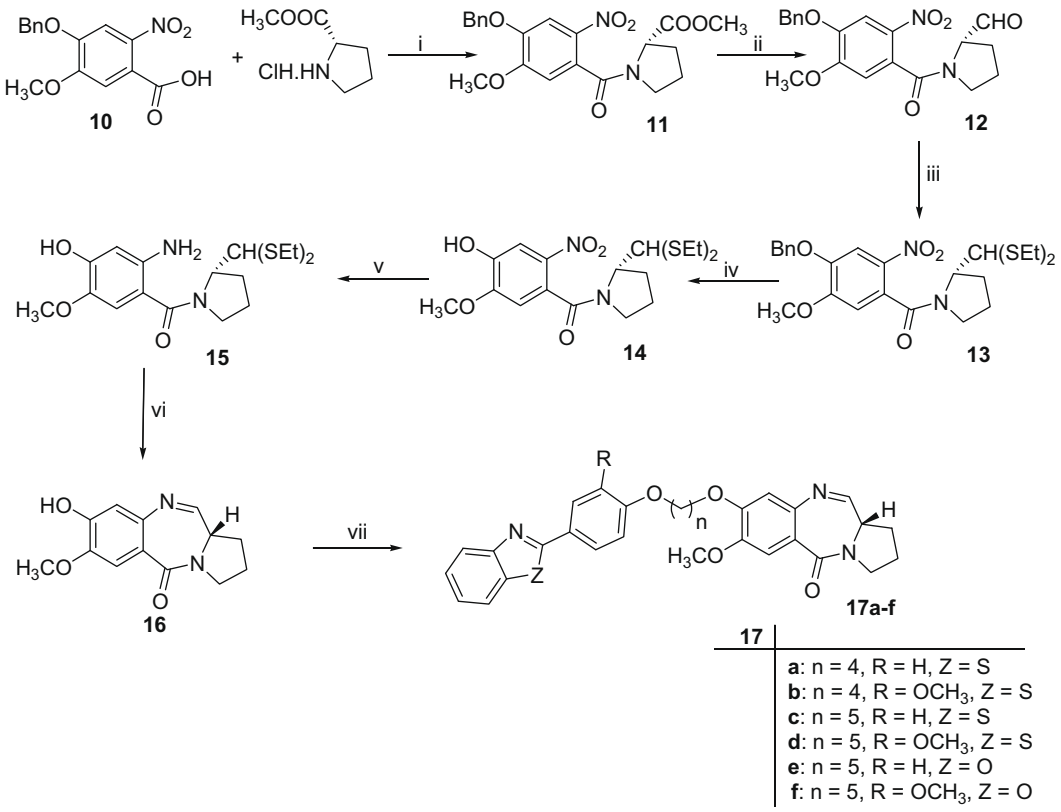

Scheme 4. Reagents and conditions: (i) (1) $SOCl_2$, benzene, rt; (2) THF, Et_3N; (ii) DIBAL-H, DCM, −70 °C; (iii) TMSCl, EtSH, DCM; (iv) EtSH, BF_3–OEt_2, CH_2Cl_2, 12 h, rt; (v) $SnCl_2{\cdot}2H_2O$, MeOH, 2 h, reflux; (vi) $HgCl_2$–$CaCO_3$, CH_3CN–H_2O (4:1); (vii) compounds **5a**–**f**, KI, K_2CO_3, acetone, 24 h.

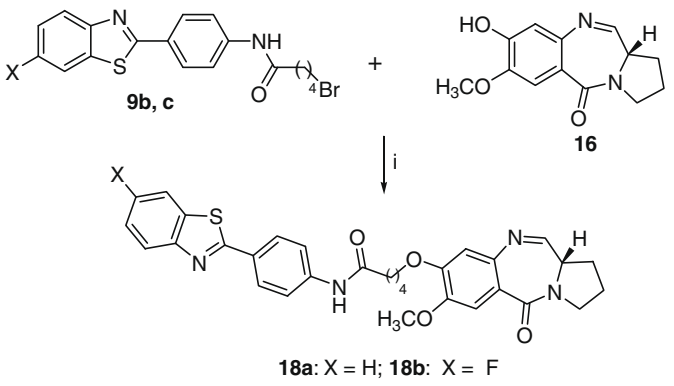

Scheme 5. Reagents and condition: (i) KI, K_2CO_3, acetone, 24 h.

DNA (5′-CGCAGAAATTTCTGCG-3′)–ligand complex from the GOLD docking has been opted for the input preparation of molecular dynamic simulations.

3.2.2. Molecular dynamic simulations

Further, more rigorous molecular dynamic simulations were employed to quantitatively understand the dynamical nature of the complex, and the interaction energy as well as assessing the effect of temperature and solvent. The effect of water as solvent was taken into account through the GBSA implicit solvent model.[21,22] The molecular dynamic results show that the minor groove of the DNA structure is preferred over the major groove and linker region of the heterodimers preferred to bind in the sequence composed mainly of adenine (A) and thymine (T) bases. Ligand binding to the DNA shows that the linker stretched over the AT region instead of making bend conformation.

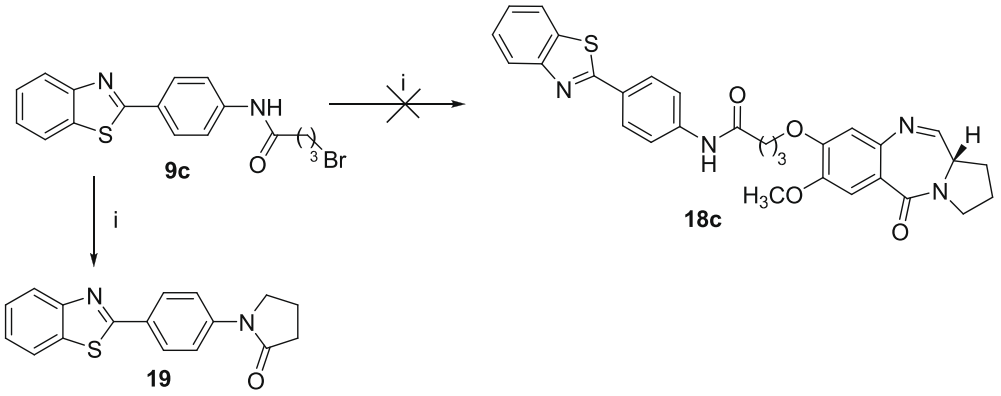

Scheme 6. Reagents and condition: (i) DC-81, KI, K_2CO_3, acetone, 24 h.

Table 1
Thermal denaturation data for benzothiazole, benzoxazole–PBD hybrids (17**a–f**, **18a,b**) with calf thymus (CT) DNA

PBD hybrids	[PBD]/[DNA] molar ratio[b]	ΔT_m[a] (°C) after incubation at 37 °C for	
		0 h	18 h
17a	1:5	0.5	0.5
17b	1:5	0.5	0.5
17c	1:5	4.1	4.3
17d	1:5	6.2	6.3
17e	1:5	4.1	4.3
17f	1:5	4.1	4.2
18a	1:5	0.5	0.5
18b	1:5	2.1	2.3
DC-81	1:5	0.3	0.7

[a] For CT-DNA alone at pH 7.00 ± 0.01, T_m = 69.1 °C ± 0.01 (mean value from 10 separate determinations), all ΔT_m values are ±0.1–0.2 °C.
[b] For a 1:5 molar ratio of [PBD]/[DNA], where CT-DNA concentration = 100 μM and ligand concentration = 20 μM in aqueous sodium phosphate buffer (10 mM sodium phosphate + 1 mM EDTA, pH 7.00 ± 0.01).

Table 2
GOLD docking fitness scores of the DNA (A)–ligand interaction

Mol	Exp. rank	Fitness	Fitness rank	vdw_ext	vdw_ext Rank	vdw_int	vdw_int Rank
17a	5	68.10	7	54.62	8	−7	8
17b	3	69.47	4	58.22	4	−10.58	3
17c	4	68.52	5	57.28	6	−10.24	5
17d	1	73.04	1	61.54	1	−11.58	2
17e		67.68	8	56.82	7	−10.46	4
17f		68.44	6	58.41	2	−11.87	1
18a	2	71.05	2	58.24	3	−9.02	6
18b		70.97	3	57.98	5	−8.76	7

3.2.3. MM-PBSA calculations

The MM-PBSA approach has emerged as a useful approach to calculate binding affinities of biomolecular complexes for distinguishing between good and weak binders, but rarely to reproduce smaller free energy differences.[23] Binding of the ligands in the minor groove does not have a large impact on the conformation of the DNA, as revealed by the qualitative (trajectory) and quantitative agreement with RMSD of the complex. In the last 500 ps (conformations in the trajectory 500–550) of 2 ns production run (conformations in the Fig. 3, 350–550) the RMSD fluctuates from the equilibrium and steady at certain level. The fluctuation in RMSD has been observed when DNA strands relaxed from the ends of the ligand binding.

In the bound structure, the molecules form interactions with the AT rich sequence of the DNA duplex, locally displace the water molecules of the spine of hydration (Fig. 4B). The different energy terms of DNA, **17d** and complex is given in Table 3. The total binding free energy ($\Delta G_{bind,solv}$) shows that the DNA–**17d** complex (−39.92 kcal/mol) is slightly more stable than other compounds (Table 4). The flanking pentameric ring of these compounds is found to be parallel with the ribose sugar of nucleotide which appears to make a π-stacking type of arrangement. The comparison between GOLD score, the binding free energy in gas and solvent phase are consistent with the experimental observations (Fig. 4).

The double bonded nitrogen of the seven-membered ring of compound **17d** interacts (~3 Å) with the N3 nitrogen of A7 and A8 nucleotide. The nitrogen of sulfur containing pentameric ring is found to be close with the A23 and A24 in the trajectory analysis. The methoxy groups of dimer always protrude out from the DNA axis. In this series of compounds, the benzothiazole shows

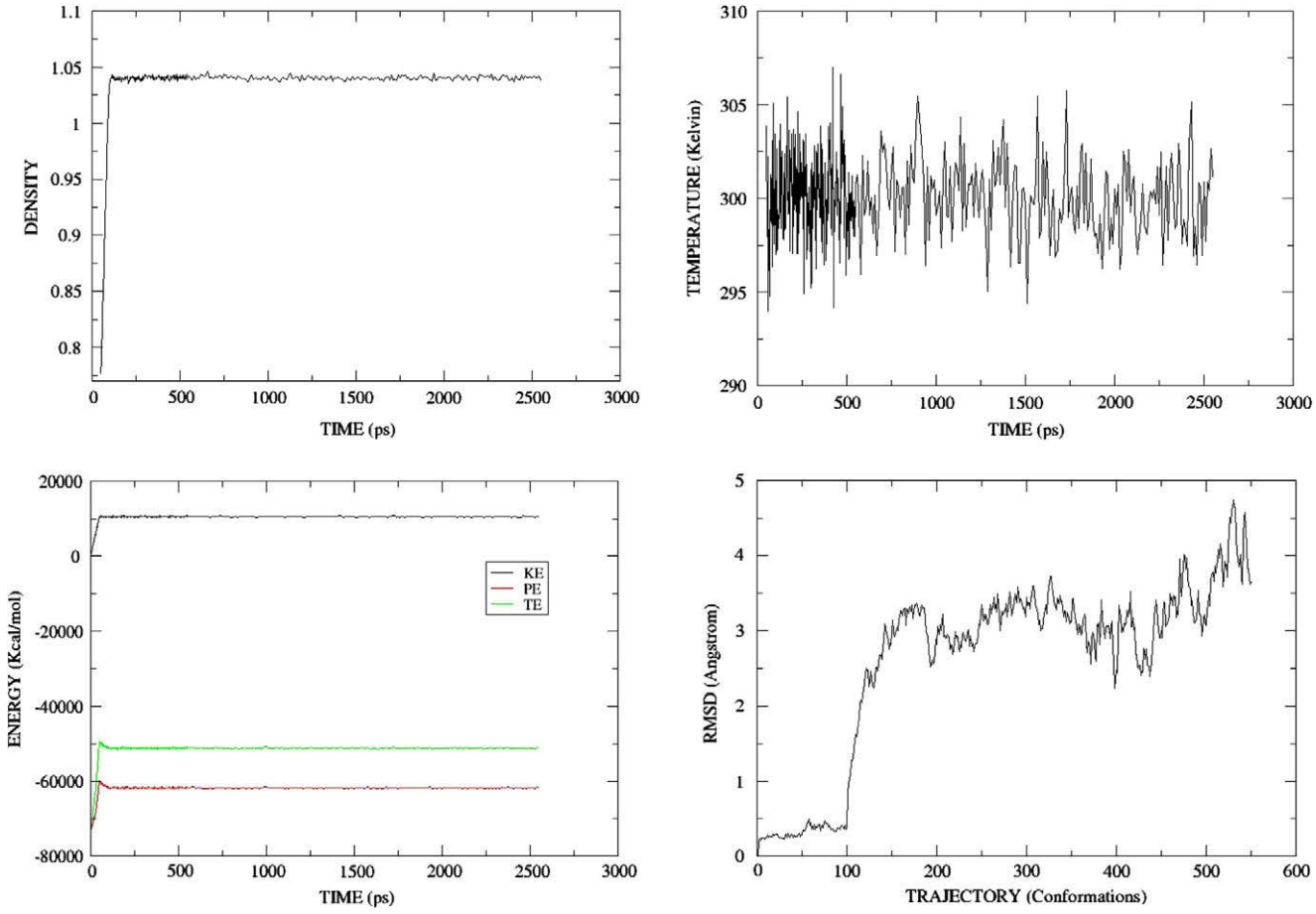

Figure 3. DNA–**17d** complex: the density, temperature, total energy and RMSD plots have all clearly converged by the end of equilibration and production period.

significantly higher binding strengths than the benzoxazole, with the DNA. It is interesting to note that the $\Delta G_{bind,solv}$ decreases as the linker length increases, indicating that the increase in the alkane spacer length from three to five enhances the stability of the DNA–ligand complex by about 9 kcal/mol (Table 4). As the covalent binding with the guanine nucleotide of AGA sequence is important for the stability of DNA–ligand complex, the longer chain length in the PBD ligands is desirable as this facilitates the ligand to come closer to guanine. Both strands of DNA come closer together when the compound is introduced in the minor groove but rest of the DNA seems to be more relaxed as depicted in Figure 4B. This partitioning of anionic charge by heterodimer into the minor groove of AT base pairs intended in the attempt toward ligand design.

3.3. In vitro anticancer activity

The C8-linked benzothiazole–PBD conjugates (**17a**–**d**, **18a**) have been evaluated against 60 human cancer cell lines derived from nine cancer cell types (leukaemia, non-small cell lung cancer, colon cancer, CNS cancer, melanoma, ovarian cancer, renal cancer, prostate cancer and breast cancer). For each compound, dose–response curves for individual cell lines have been measured at a minimum of five concentrations at 10-fold dilutions. A protocol of 48 h continuous drug exposure has been used, and a sulforhodamine B (SRB) protein assay was used to estimate cell viability or growth (Table 5).[24] Specifically, compound **17d** has exhibited excellent cytotoxicity against all tested leukaemia cell lines and also against Hop-62, Hop-92, NCI-H23, NCI-H460, NCI-H522 (non-small cell lung cancer), COLO 205, HT-116, HT29, SW-620 (colon cancer), SF-295, SF-539, U251 (CNS cancer), LOX IMVI, M14, SK-MEL-5, UACC-62 (melanoma cancer), prostate, some of the renal, breast and ovarian cell lines in the range of 15–25 nM. While the other compounds (**17a**–**c**) have also shown significant anticancer activity in the sub-micromolar range against all the cell lines tested. Interestingly, the amide derivative **18a** has shown comparatively less activity than the corresponding ether derivatives. It is noticed that the acetylated benzothiazoles[7a] which are more active towards breast cancer cell lines have not retained their activity in benzothiazole–pyrrolobenzodiazepine conjugates (**18a**).

3.4. Cell cycle effects in A375 cells

The anticancer activity data has revealed that these compounds **17b**, **17d** and **18a** caused pronounced and efficient cytotoxicity against 60 cancer cell lines tested, among the above, compound **17d** was found to be highly effective in causing cytotoxicity. These results prompted us to investigate the effect of these compounds on cell cycle progression and apoptosis in A375 human melanoma cancer cell line by using DC-81 as positive control. The optimized

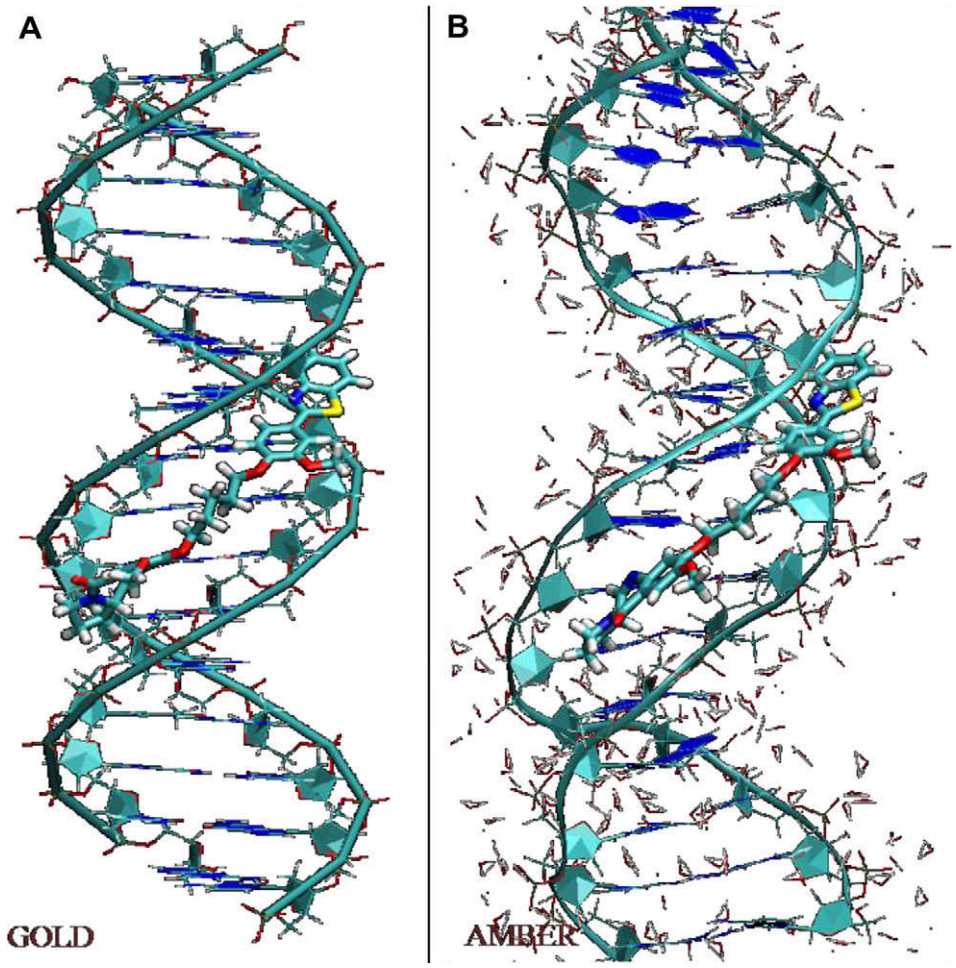

Figure 4. GOLD docking and MD trajectory pose of DNA(A)–ligand (**17d**) complex: (A) binding of ligand in the minor groove of DNA as observed in GOLD docking. (B) Distortions of the double helix of DNA on the binding of ligand observed on molecular dynamics simulation of the docked pose revealing the local displacement of water molecules of the spine of hydration and the effect of binding of inhibitor on DNA conformation showing the uncoiling of the DNA helix from the sites flanking the bound inhibitor, in contrast to the shrinking tendency exhibited by the region of DNA strands bound by the inhibitor may be due to non-covalent interaction.

Table 3
Calculated interaction energy and solvation free energy for complex (DNA + **17d**) and average the results to obtain an estimate of the final binding free energy ($\Delta G_{bind,solv}$) contributions of all the snapshots from the complex trajectory using MM-PBSA

Component	Complex		Receptor		Ligand		$\Delta G_{bind,solv}$	
	Mean	STD	Mean	STD	Mean	STD	Mean	STD
ELE	2444.83	62.87	2471.02	62.64	−2.63	1.1	−23.56	4.39
VDW	−346.37	12.35	−291.07	11.28	18.98	2.19	−74.28	2.94
INT	1598.82	23.98	1506.53	23.32	92.29	6.34	0.00	0.00
GAS	3697.28	61.91	3686.48	61.3	108.64	6.04	−97.84	5.65
GBSUR	44.57	0.28	45.57	0.23	6.91	0.05	−7.91	0.19
GBTOT	−9606.59	57.64	−9633.17	57.56	−28.68	0.72	55.26	4.05
GBSOL	−9562.02	57.73	−9587.61	57.63	−21.76	0.7	47.35	3.98
GBELE	−7161.76	14.79	−7162.15	14.53	−31.31	0.86	31.7	1.8
GBTOT	−5864.75	23.08	−5901.13	21.95	86.87	5.92	−50.49	2.95
PBSUR	44.57	0.28	45.57	0.23	6.91	0.05	−7.91	0.19
PBCAL	−9833.25	58.02	−9868.87	58.1	−30.21	0.79	65.82	4.79
PBSOL	−9788.68	58.11	−9823.3	58.19	−23.29	0.76	57.92	4.7
PBELE	−7388.42	14.85	−7397.84	14.05	−32.84	0.72	42.26	3.87
PBTOT	−6091.4	23.24	−6136.82	21.63	85.34	5.91	−39.92	4.23

All values are in kcal/mol.
ELE: electrostatic energy; VDW: van der Waals energy; INT: internal energy (this term always amounts to zero in the single trajectory approach); GAS: total gas-phase energy (sum of ELE, VDW and INT); PBSUR/GBSUR: non-polar contribution to the solvation free energy calculated by an empirical model; PBCAL/GB: electrostatic contribution to the solvation free energy calculated by PB or GB, respectively; PBSOL/GBSOL: sum of non-polar and polar contributions to salvation; PBELE/GBELE: sum of the electrostatic solvation free energy and MM electrostatic energy; PBTOT/GBTOT: final estimated binding free energy.

Table 4
Calculated free binding energy (kcal/mol) of DNA (A)–ligand interaction using MM-PBSA method (AMBER)[a]

Component	Binding free energy $\Delta G_{bind,solv}$				
	17a	**17b**	**17c**	**17d**	**18a**
ELE	−12.93	−20.25	−20.57	−23.56	−28.81
VDW	−68.69	−67.45	−73.54	−74.28	−67.92
INT	0.00	0.00	0.00	0.00	0.00
GAS	−81.62	−87.7	−94.11	−97.84	−96.73
GBSUR	−7.20	−7.24	−7.76	−7.91	−7.26
GB	44.89	49.91	51.98	55.26	58.35
GBSOL	37.70	42.66	44.22	47.35	51.09
GBELE	31.97	29.66	31.41	31.70	29.53
GBTOT	−43.92	−45.04	−49.89	−50.49	−45.64
PBSUR	−7.20	−7.24	−7.76	−7.91	−7.26
PBCAL	58.16	57.69	65.54	65.82	65.71
PBSOL	50.96	50.45	57.78	57.92	58.45
PBELE	45.24	37.44	44.97	42.26	36.90
PBTOT	−30.65	−37.26	−36.33	−39.92	−38.28

[a] For the definition of these terms refer to footnote in Table 3.

concentration, at which good apoptotic events occur, was found to be at 2 μM (Table 6.1). Subsequently, these compounds were tested at 2 μM concentration, and the percentage of G0/G1 phase cells were found to be 54.55, 77.93, 90.55, 93.79 and 88.44 for control, DC-81, **17b**, **17d** and **18a**, respectively (Figs. 5.1 and 5.2).

An increase in the percentage of cells in the G0 phase was observed which indicated the cells have undergone programmed cell death (apoptosis) for all the tested compounds (Fig. 5.3). Compound **17d** was found to be the most effective one among the tested conjugates. Increase of apoptotic cells (G0 cells) with increase of concentration (0–2 μM) of compounds (DC-81 and **17d**) was observed and this increase was found to be synergistic (Fig. 5.4). The different phases of cell cycle were analyzed and the results are summarized in Table 6.2.

3.5. In vivo tumour xenograft studies of 17d

The preliminary in vitro anticancer activities, thermal denaturation and FACS studies revealed that compound **17d** has shown significant anticancer activity among the series. These encouraging results provided an impetus to carry out in vivo efficacy studies using xenograft model of human colon cancer cells (HT29) in male *scid* mice. The dose determination studies demonstrated the maximum tolerated dose of compound **17d** as <50 mg/Kg. Hence, compound **17d** was administered at 5 mg/kg and 10 mg/kg, intraperitoneal (ip), on days 1, 5 and 9 (q4d) (total drug administered was 15 and 30 mg/kg, respectively). With these doses no toxicity was observed in terms of weight loss or mortality of the experimental mice (Fig. 6i and ii). The tumour volume, body weight and signs of overt toxicity following test compound dosing were monitored and recorded for the duration of the experiment (35 days). Tumour growth was expressed in terms of relative tumour volume (RTV) (Fig. 6iii) which is the ratio of tumour volume on a particular day to the tumour volume on day 1 of the study. Tumour growth inhibition index T/C (Fig. 6iv) was calculated as follows:

T/C = Average RTV of test group mice/Average RTV of control group mice.

The T/C data demonstrated that administration of **17d** under the above conditions did not cause significant inhibition of tumour weight relative to the vehicle control during the period of experiment (35 days). However, a trend of tumour inhibition was observed with a minimum T/C value of 0.58 was attained on day 21 in the 30 mg/kg treatment group. Probably metabolic instability or poor bioavailability is responsible for limiting the in vivo efficacy. Current studies are ongoing to understand the metabolism and distribution of this series and to design newer generation of compounds with more stability and bioavailability aspects.

4. Conclusion

In conclusion, the synthesis and DNA-binding affinity of new C8-linked benzothiazole/benzoxazole–PBD conjugates attached through varying alkane and alkylamide spacers have been investigated. Among the four PBD conjugates evaluated, conjugate **17d** has shown pronounced in vitro anticancer activity against 60 human tumour cell lines. Molecular modelling studies suggest that the sulfur atom in benzothiazole ring system and an increase of the linker length to a five-carbon chain significantly enhances the DNA-binding ability of the minor groove binders with the DNA sequence A. The MD simulations using MM-PBSA methodologies provide valuable insights in the ligand DNA binding. Further, the effect of these compounds on cell cycle progression was studied with PBD conjugates such as **17b**, **17d**, **18a** and DC-81 against A375 cell

Table 5
Anticancer activity of benzothiazole–pyrrolo[2,1-*c*][1,4]benzodiazepine conjugates (**17a–d**, **18a**) in human cancer cell lines

Panel/cell line	Growth inhibition $Log_{10}GI_{50}$ (M)				
	17a	**17b**	**17c**	**17d**	**18a**
Leukaemia					
CCRF-CEM	−6.55	−6.47	−6.57	−7.66	−5.92
HL-60 (TB)	−6.42	−6.29	−6.25	−7.48	−5.75
K-562	−6.45	−6.47	−6.44	−7.69	−5.76
MOLT-4	−6.63	−6.17	−6.55	−7.36	−5.79
RPMI-8226	−6.67	−6.51	−6.40	−7.13	−5.84
SR	−7.66	−6.53	−7.72	−7.76	−6.26
Non-small cell lung cancer					
A549/ATCC	−5.58	−5.57	−5.59	−6.62	−5.47
EKVX	−5.90	−5.76	−5.81	−6.69	−5.61
HOP-62	−6.39	−5.85	−6.39	−7.34	−5.61
HOP-92	−6.75	−6.58	−6.57	−7.35	−5.76
NCI-H226	−5.84	−5.62	−5.82	−6.67	−5.54
NCI-H23	−6.13	−5.83	−6.05	−7.21	—
NCI-H322M	−5.66	−5.59	−5.71	−6.52	−5.55
NCI-H460	−6.39	−6.19	−6.46	−7.40	−5.78
NCI-H522	−6.49	−6.26	−6.26	−7.38	−6.01
Colon cancer					
COLO 205	−6.47	−6.16	−6.41	−7.22	−5.77
HCC-2998	−6.44	−6.19	−6.20	−6.90	−5.80
HCT-116	−6.53	−6.28	−6.46	−7.41	−5.73
HCT-15	−6.19	−5.88	−6.03	−6.65	−5.55
HT29	−6.42	−6.27	−6.34	−7.39	−5.67
KM12	−6.26	−5.99	−5.81	−6.78	−5.53
SW-620	−6.37	−6.10	−5.99	−7.25	−5.79
CNS cancer					
SF-268	−6.18	−5.91	−5.49	−6.46	−5.69
SF-295	−6.17	−5.72	−6.11	−7.17	−6.26
SF-539	−6.46	−6.27	−6.32	−7.40	−5.80
SNB-19	−5.82	−5.79	−5.53	−6.66	−5.57
SNB-75	−5.97	−5.91	−5.92	−6.84	−5.74
U251	−6.64	−6.38	−6.34	−7.47	−5.72
Melanoma					
LOX IMVI	−6.39	−6.14	−6.62	−7.74	−5.81
MALME 3M	−5.90	−5.81	−5.91	−6.84	−5.72
M14	−6.27	−5.91	−6.49	−7.40	−5.81
SK-MEL-2	−6.41	−5.91	−5.81	−6.75	−5.71
SK-MEL-28	−5.67	−5.67	−5.41	−6.48	−5.65
SK-MEL-5	−6.46	−6.39	−6.47	−7.61	−5.75
UACC-257	−5.66	−5.66	−5.65	−6.73	−5.76
UACC-62	−6.10	−5.95	−5.93	−7.09	−5.76
Ovarian cancer					
IGROV1	−5.62	−5.51	−5.57	−6.46	−6.16
OVCAR-3	−6.42	−6.14	−6.13	−7.01	−5.73
OVCAR-4	−5.94	−5.79	−5.67	−6.54	−5.55
OVCAR-5	−6.48	−6.30	−6.18	−7.15	−5.45
OVCAR-8	−6.12	−5.75	−6.09	−6.85	−5.81
SK-OV-3	−5.91	−5.62	−5.59	−6.75	−5.35
Renal cancer					
786-0	−6.67	−6.05	−6.58	−7.56	−5.81
A498	−5.69	−5.79	−5.65	−6.76	−5.73
ACHN	−6.44	−6.11	−5.96	−7.27	−5.52
CAKI-1	−6.45	−6.24	−6.29	−6.93	−5.66
RXF 393	−6.72	−6.62	−6.70	−7.29	−5.79
SN12C	−6.20	−6.02	−6.09	−6.70	−5.55
TK-10	−6.32	−5.82	−5.46	−6.48	−5.49
UO-31	−6.18	−5.91	−6.14	−6.70	−5.78
Prostate cancer					
PC-3	−6.53	−6.39	−6.63	−7.38	−5.69
DU-145	−6.57	−6.52	−6.45	−7.47	—
Breast cancer					
MCF-7	−6.49	−6.39	−6.48	−7.72	−6.14
NCI/ADR-RES	−5.94	−5.72	−5.95	−6.57	−4.96
MDA-MB-231/ATCC	−6.57	−6.28	−6.58	−7.05	−5.68
HS 578T	−6.30	−5.99	−5.88	−6.85	−5.56
MDA-MB-435	−6.35	−5.87	−5.86	−7.07	−5.75
BT-549	−6.74	−6.55	−6.64	−7.66	−5.95
T-47D	−6.66	−6.59	−6.63	−7.85	−5.71
MG_MID	−6.30	−6.07	−6.15	−7.09	−5.72

Table 6.1
Cell cycle distribution of A375 cell line using **17b**, **17d**, **18a** and DC-81 at 2 μM concentrations

Compound	Concn (μM)	Cell cycle distribution (%)			
		G0	G1	S	G2/M
Control	0	0.99	53.56	15.93	29.52
17b	2	20.86	69.69	5.00	4.45
17d	2	26.75	67.04	3.11	3.10
18a	2	15.10	73.34	6.15	5.41
DC-81	2	10.70	67.23	13.54	8.53

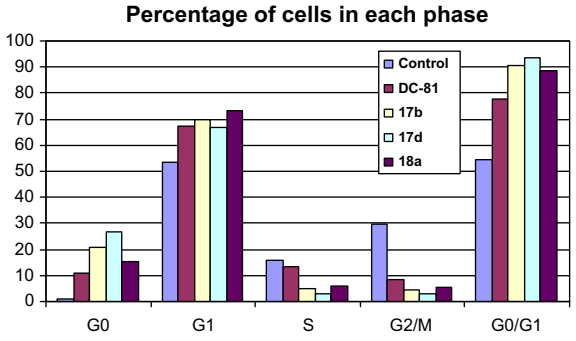

Figure 5.1. Flow cytometric analysis for the cell cycle distribution of A375 cells after exposure to hybrids **17b**, **17d**, **18a** and DC-81 (2 μM) for 24 h (G0 = apoptotic sub-G1 area; G1 area; S area; G2/M area).

line and **17d** was found to be most effective at a low concentration of 0.5 μM which is indicated by the increase of sub-G1 apoptotic cells. The order of effect of these compounds in causing apoptosis is **17d** > **17b** > **18a** > DC-81. The in vivo efficacy study of compound **17d** revealed that the ability to delay the tumour growth and retention of body weight apart from no other adverse side-effects in the HT29 human colon cancer xenograft model suggested that PBD-bezothiazole/benzoxazole conjugates have promising anti-cancer activity in the treatment of human cancer.

5. Experimental

5.1. General

^{1}H NMR spectra were recorded on a Bruker UXNMR/XWIN-NMR (300 MHz) or Varian VXR-Unity (200 MHz). Chemical shifts have been expressed in (ppm) down field from TMS. Coupling constants are reported in hertz (Hz). EI mass spectra were recorded on a VG-7070H Micromass mass spectrometer at 200 °C, 70 eV, with a trap current of 200 μA and 4 kV of acceleration voltage. FAB mass spectra were recorded on a LSIMS-VG-AUTOSPEC Micromass spectrometer. LC mass spectra and ESI mass spectra were recorded on LC-MSD-Trap-SL spectrometer and Q-STAR-XL Hybrid spectrometer, respectively. Elemental analysis was within ±0.4% of the theoretical values. All reactions were monitored by thin-layer chromatography (TLC) carried out on 0.25 mm E. Merck silica gel plates (60F-254) with UV light, iodine as probing agents. Column chromatography was performed using Acme silica gel (100–200 mesh). Yields were not optimized. All solvents and reagents were used without further purification unless otherwise specified.

5.2. General procedures

5.2.1. 2-[4-(Benzyloxy)phenyl]-1,3-benzoxazole (2a)

A mixture of 2-aminophenol (545 mg, 5 mmol) and 4-benzyloxy benzaldehyde (1.06 g, 5 mmol) was refluxed in ethanol

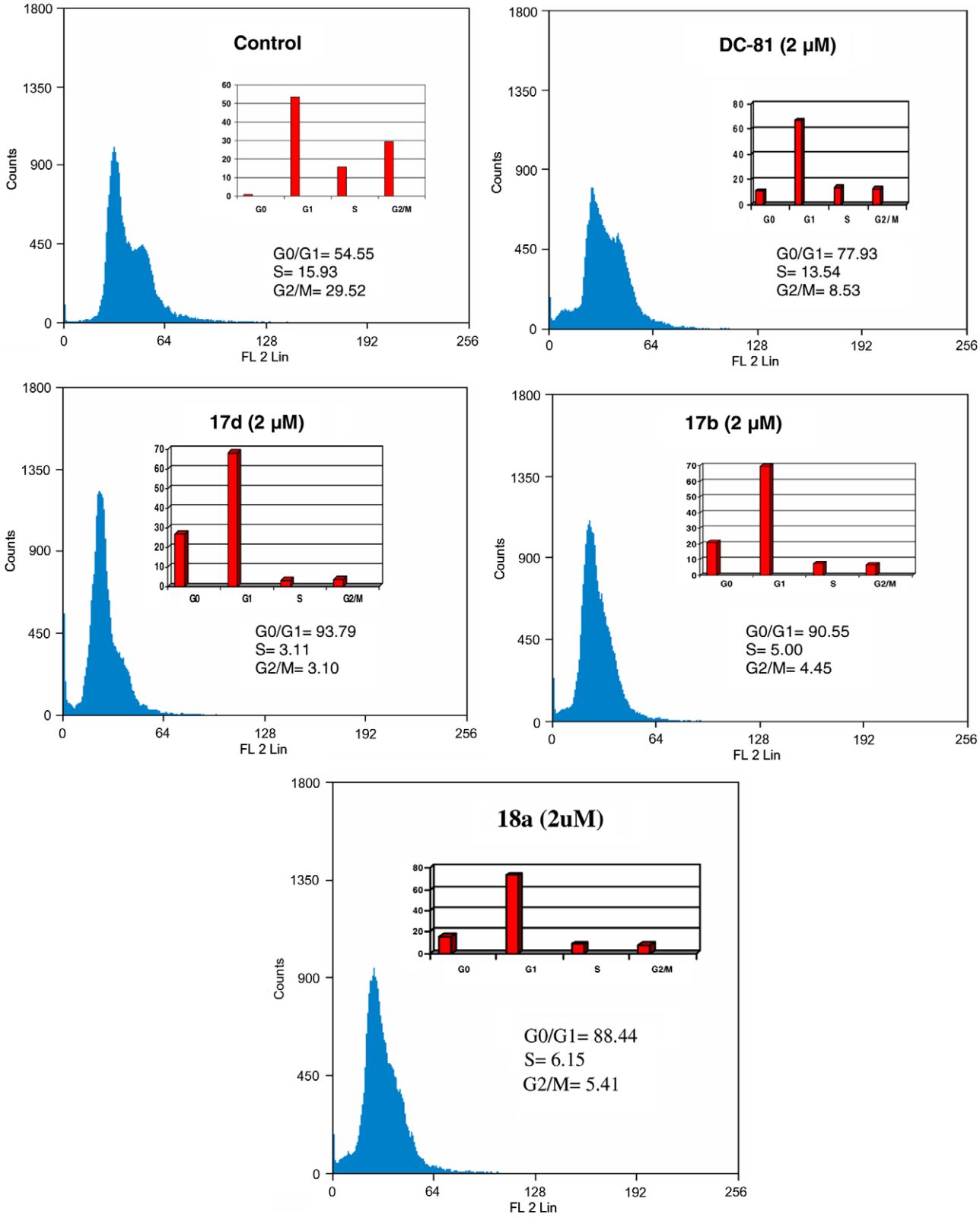

Figure 5.2. FACS analysis of cell cycle distribution of A375 cells after treatment with benzothiazole/benzoxazole–pyrrolo[2,1-*c*][1,4]benzodiazepine conjugates at 2 μM concentration for 24 h. DC-81 was used as the positive control. Control: cells treated with DMSO.

(35 mL). After few minutes, a yellow precipitate was observed. The obtained precipitate **1a** was filtered and used without further purification (1.2 g, 80%). The product **1a** (500 mg, 1.65 mmol) was dissolved in chloroform (20 mL). To this solution, 1.1 g of lead tetra acetate (2.5 mmol) was added in portionwise. The resulting mixture was refluxed for about 1 h. After cooling to room temperature, the reaction mixture was filtered and concentrated under reduced pressure. The residue thus obtained was purified by column

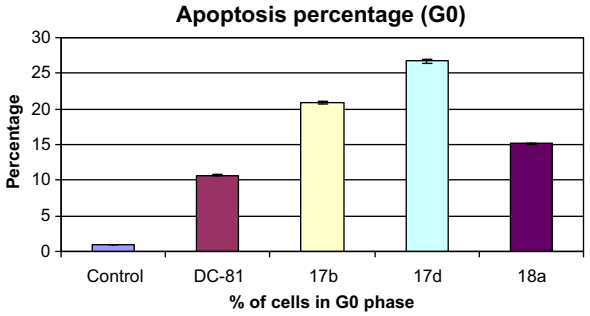

Figure 5.3. Apoptosis percentage of A375 cells treated with compounds **17b**, **17d**, **18a** and DC-81 at 2 μM concentration.

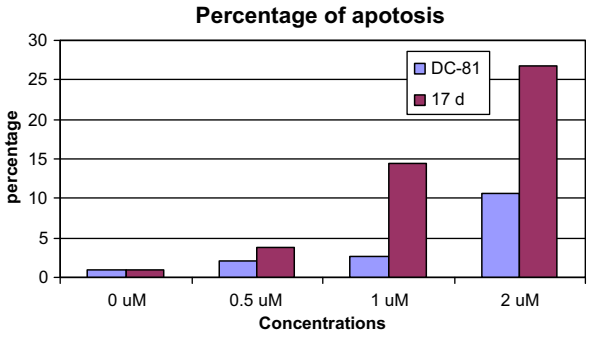

Figure 5.4. Comparative study of apoptosis in A375 cells treated with compound DC-81 and **17d**. The percentages of accumulation of sub-G0 phase cells of the positive control (DC-81) and compound **17d** (0.5, 1 and 2 μM) were 2.13%, 2.23%; 2.7%, 14.41%; and 10.7%, 26.75%, respectively.

Table 6.2
Cell cycle distribution of A375 cell line with variable concentration of the **17d** and DC-81 (0, 0.5, 1 and 2 μM) compounds

Compound	Concn (μM)	Cell cycle distribution (%)				
		G0	G1	S	G2/M	G0/G1
Control	0	0.99	53.56	15.93	29.52	54.55
DC-81	0.5	2.13	64.95	16.96	15.96	67.08
17d	0.5	3.73	79.42	10.40	6.45	83.15
DC-81	1	2.70	61.56	15.42	20.32	64.26
17d	1	14.41	74.22	5.03	6.34	88.63
DC-81	2	10.70	67.23	13.54	8.53	77.93
17d	2	26.75	67.04	3.11	3.10	93.79

chromatography using ethyl acetate and hexane (5:95) as eluant affords compound **2a** as a brown solid (350 mg, 70%). ^{1}H NMR ($CDCl_3$, 300 MHz): δ 8.22 (d, 2H, J = 9.0 Hz), 7.68–7.72 (m, 1H), 7.44–7.52 (m, 1H), 7.27–7.51 (m, 7H), 7.12 (d, 2H, J = 9.0 Hz), 5.20 (s, 2H); ESIMS: m/z 302 (M^++1).

5.2.2. 2-[4-(Benzyloxy)-3-methoxyphenyl]-1,3-benzoxazole (2b)

The compound **2b** was prepared according to the method described for **2a** by employing 2-aminophenol (545 mg, 5 mmol) and 4-benzyloxy-3-methoxybenzaldehyde (1.2 g, 5 mmol) followed by oxidative cyclization with lead tetra acetate affords compound **2b** as light brown coloured solid (yield 70%). ^{1}H NMR ($CDCl_3$, 300 MHz): δ 7.62–7.78 (m, 3H), 7.24–7.55 (m, 8H), 6.95 (d, 1H, J = 8.5 Hz), 5.20 (s, 2H), 4.02 (s, 3H); ESIMS: m/z 332 (M^++1).

5.2.3. 4-(1,3-Benzoxazol-2-yl)phenol (3a)

To a solution of **2a** (250 mg, 0.82 mmol) in ethyl acetate (20 mL) under hydrogen atmosphere, was added 10% Pd/C (87 mg, 0.082 mmol). The resulting mixture was stirred at room temperature for about 1 h. After this time, the reaction mixture was filtered and concentrated under reduced pressure. The residue thus obtained was purified by column chromatography using ethyl acetate and hexane (1:9) as eluant affords compound **3a** as light brown colour solid (165 mg, 95%). ^{1}H NMR ($CDCl_3$, 300 MHz): δ 8.08 (td, 2H, J = 8.5, 2.3 Hz), 7.62–7.68 (m, 1H), 7.53 (m, 1H), 7.25–7.31 (m, 2H), 6.92 (td, 2H, J = 8.5, 2.3 Hz); ESIMS: m/z 212 (M^++1).

5.2.4. 4-(1,3-Benzoxazol-2-yl)-2-methoxyphenol (3b)

The compound **3b** was prepared according to the method described for **3a** by employing **2b** (250 mg, 0.75 mmol) and Pd/C (0.075 mmol) (yield 172 mg, 95%). ^{1}H NMR ($CDCl_3$, 300 MHz): δ 7.66–7.83 (m, 3H), 7.50–7.55 (m, 1H), 7.25–7.32 (m, 2H), 7.03 (d, 1H, J = 7.8 Hz), 5.95 (br s, 1H, exchangable with DMSO-d_6), 4.05 (s, 3H); ESIMS: m/z 242 (M^++1).

5.2.5. 2-[4-(4-Bromobutyloxy)-phenyl]-1,3-benzothiazole (5a)

To a solution of compound **4a** (227 mg, 1 mmol) in dry acetone (15 mL) was added, anhydrous K_2CO_3 (553 mg, 4 mmol), 1,4-dibromobutane (324 mg, 1.5 mmol) and the reaction mixture was stirred at reflux temperature for 48 h. the reaction mixture was monitored by TLC. After completion of the reaction as indicated by TLC, K_2CO_3 was removed by filtration and the solvent was evaporated under reduced pressure, diluted with water and extracted with ethyl acetate. The combined organic phases were dried over Na_2SO_4 and evaporated under vacuum. The residue, thus obtained was purified by column chromatography using ethyl acetate and hexane (2:8) to afford compound **5a** as white solid (340 mg, 95%). ^{1}H NMR ($CDCl_3$, 300 MHz); δ 7.90–7.98 (m, 3H, J = 9.0 Hz), 7.83 (d, 1H, J = 7.5 Hz), 7.42 (d, 1H, J = 8.3 Hz), 7.30 (d, 1H, J = 7.5 Hz), 6.94 (d, 2H, J = 9.0 Hz), 4.2 (t, 2H, J = 6.0 Hz), 3.58 (t, 2H), 1.5–2.1 (m, 4H); EIMS: m/z 363 (M^++1).

5.2.6. 2-[4-(4-Bromobutyloxy)-2-methoxyphenyl]-1,3-benzothiazole (5b)

The compound **5b** was prepared according to the method described for **5a** by employing hydroxyl benzothiazole (**4b**) (257 mg, 1 mmol) and 1,4-dibromobutane (324 mg, 1.5 mmol) as a white coloured solid (yield 372 mg, 96%).

^{1}H NMR ($CDCl_3$, 300 MHz); δ 7.98 (d, 1H, J = 8.3 Hz), 7.83 (d, 1H, J = 7.5 Hz), 7.67 (s, 1H), 7.52 (dd, 1H, J = 7.5, 2.5 Hz), 7.44 (t, 1H, J = 7.5 Hz), 7.32 (t, 1H, J = 7.5 Hz), 6.91 (d, 1H, J = 8.3 Hz), 4.2 (t, 2H, J = 6.0 Hz), 3.92 (s, 3H), 3.58 (t, 2H), 2.1 (m, 4H); EIMS: m/z 393 (M^++1).

5.2.7. 2-[4-(5-Bromopentyloxy)-phenyl]-1,3-benzothiazole (5c)

The compound **5c** was prepared according to the method described for **5a** by employing hydroxyl benzothiazole (**4a**) (227 mg, 1 mmol) and 1,5-dibromopentane (345 mg, 1.5 mmol) as a white colour solid (yield 360 mg, 96%).

^{1}H NMR ($CDCl_3$, 300 MHz); δ 7.90–7.98 (m, 3H, J = 9.0 Hz), 7.83 (d, 1H, J = 7.5 Hz), 7.42 (d, 1H, J = 8.3 Hz), 7.30 (d, 1H, J = 7.5 Hz), 6.94 (d, 2H, J = 9.0 Hz), 4.2 (t, 2H, J = 6.0 Hz), 3.43 (t, 2H, J = 6.0 Hz), 1.97 (q, 2H, J = 7.5 Hz), 1.87 (q, 2H, J = 7.3 Hz), 1.72–1.63 (m, 2H); EIMS: m/z 377 (M^++1).

5.2.8. 2-[4-(5-Bromopentyloxy)-2-methoxyphenyl]-1,3-benzothiazole (5d)

The compound **5d** was prepared according to the method described for **5a** by employing hydroxyl benzothiazole (**4b**) (257 mg, 1 mmol) and 1,5-dibromopentane (345 mg, 1.5 mmol) as a white coloured solid (yield 380 mg, 96%).

^{1}H NMR ($CDCl_3$, 300 MHz); δ 7.98 (d, 1H, J = 8.3 Hz), 7.83 (d, 1H, J = 7.5 Hz), 7.67 (s, 1H), 7.52 (dd, 1H, J = 7.5, 2.5 Hz), 7.44 (t, 1H, J = 7.5 Hz), 7.32 (t, 1H, J = 7.5 Hz), 6.91 (d, 1H, J = 8.3 Hz), 4.2 (t, 2H, J = 6.0 Hz), 3.94 (s, 3H), 3.43 (t, 2H, J = 6.0 Hz), 1.97 (q, 2H,

(i)

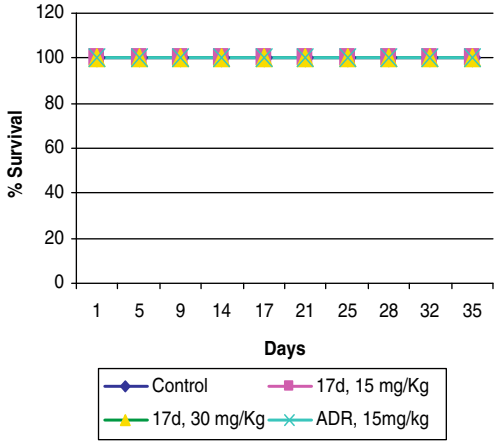

(ii)

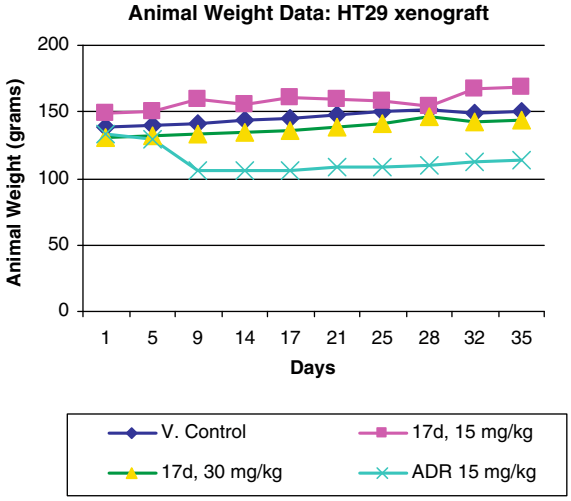

(iii)

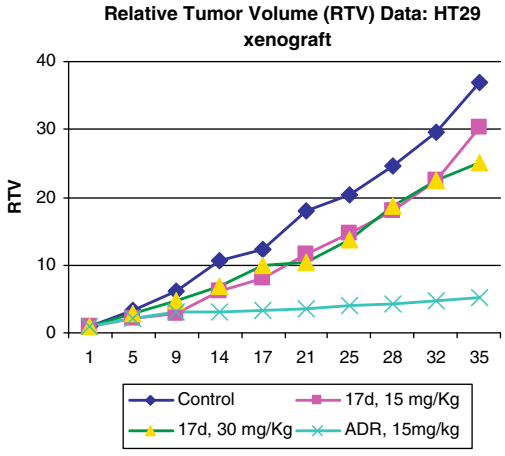

(iv)

Days	*T/C		
	17d, 15 mg/Kg	17d, 30 mg/Kg	ADR, 15mg/kg
1	1	1	
5	0.65	0.85	0.62
9	0.49	0.78	0.49
14	0.58	0.66	0.30
17	0.65	0.81	0.28
21	0.65	0.58**	0.20
25	0.72	0.67	0.20
28	0.73	0.75	0.18
32	0.76	0.76	0.16
35	0.82	0.68	0.14

Figure 6. (i) *Scid* mice treated with **17d**, Survival data of compound **17d** on HT29 xenograft mice. (ii) tumour weight curves in *scid* mice treated with **17d**. (iii) Relative tumour volume (RTV), T/C values derived from RTV data, *T/C ⩽ 0.2 indicates activity (values in red colour in the above table), **minimum T/C attained by compound **17d**, ADR = adriamycin (doxorubicin).

J = 7.5 Hz), 1.87 (q, 2H, *J* = 7.3 Hz), 1.72–1.63 (m, 2H); EIMS: *m/z* 407 (M^++1).

5.2.9. 2-[4-(5-Bromopentyloxy)-phenyl]-1,3-benzoxazole (5e)

The compound **5e** was prepared according to the method described for **5a** by employing hydroxyl benzoxazole (**3a**) (211 mg, 1 mmol) and 1,5-dibromopentane (345 mg, 1.5 mmol) as a white coloured solid (yield 340 mg, 96%).

^{1}H NMR ($CDCl_3$, 300 MHz); δ 8.02 (d, 2H, *J* = 9.0 Hz), 7.73 (d, 1H, *J* = 9.0 Hz), 7.50 (d, 1H, *J* = 9.0 Hz), 7.29 (m, 2H, *J* = 9.0 Hz), 6.98 (d, 2H, *J* = 8.3 Hz), 4.2 (t, 2H, *J* = 6.0 Hz), 3.43 (t, 2H, *J* = 6.0 Hz), 1.97 (q, 2H, *J* = 7.5 Hz), 1.87 (q, 2H, *J* = 7.3 Hz), 1.72–1.63 (m, 2H); EIMS: *m/z* 361 (M^++1).

5.2.10. 2-[4-(5-Bromopentyloxy)-2-methoxyphenyl]-1,3-benzoxazole (5f)

The compound **5d** was prepared according to the method described for **5f** by employing hydroxyl benzoxazole (**3b**) (241 mg, 1 mmol) and 1,5-dibromopentane (345 mg, 1.5 mmol) as a white colour solid (yield 370 mg, 96%).

^{1}H NMR ($CDCl_3$, 300 MHz); δ 7.77 (d, 1H, *J* = 8.30 Hz), 7.67–7.73 (m, 3H, *J* = 9.0 Hz), 7.52 (d, 1H, *J* = 9.0 Hz), 6.96 (d, 2H, *J* = 8.3 Hz), 4.2 (t, 2H, *J* = 6.0 Hz), 3.94 (s, 3H), 3.43 (t, 2H, *J* = 6.0 Hz), 1.97 (q, 2H, *J* = 7.5 Hz), 1.87 (q, 2H, *J* = 7.3 Hz), 1.72–1.63 (m, 2H); EIMS: *m/z* 390 (M^++1).

5.2.11. *N*1-(4-Fluorophenyl)-4-nitrobenzamide (6a)

A mixture of 4-fluoroaniline (556 mg, 5 mmol) and 4-nitrobenzoyl chloride 927.5 mg, 5 mmol) in pyridine (20 mL) was stirred under reflux. After completion of reaction, the reaction mixture was poured into water (100 mL). The precipitate was collected and washed with water (2 × 50 mL), ice-cold methanol (2 × 20 mL) to afford compound **6a** (1.24 g, 95%). ^{1}H NMR ($CDCl_3$, 300 MHz): δ 8.33 (d, 2H, *J* = 8.6 Hz), 8.09 (d, 2H, *J* = 8.6 Hz), 7.66 (m, 2H, *J* = 4.7 Hz), 7.07 (t, 2H, *J* = 8.6 Hz); EIMS: *m/z* 260 (M^+).

5.2.12. *N*1-(4-Fluorophenyl)-4-nitro-1-benzenecarbothioamide (7a)

A mixture of nitrobenzanilide (**6a**, 1 g, 3.84 mmol) and Lawesson's reagent (775.7 mg, 1.92 mmol) in HMPA (10 mL)

was stirred at 100 °C for 6 h and poured into water (100 mL). The precipitate was collected, washed with water and then ice-cold methanol to afford **7a** (955 mg, 90%). ^{1}H NMR (DMSO-d_6 + $CDCl_3$, 200 MHz): δ 11.78 (br s, 1H), 8.26 (d, 2H, J = 8.8 Hz), 8.02 (d, 2H, J = 8.8 Hz), 7.89 (m, 2H), 7.13 (t, 2H, J = 8.8 Hz); EIMS: m/z 276 (M^+).

5.2.13. 4-(6-Fluoro-1,3-benzothiazol-2-yl)aniline (8a)

The fluoro substituted nitrothiobenzanilide **7a** (900 mg, 3.25 mmol) was dissolved in a solution of NaOH (1.3 g, 32.5 mmol) in water (30 mL) and ethanol (3 mL). The mixture was added dropwise to a solution of potassium ferricyanide (13 mmol) in water (20 mL) at 90 °C, stirred for 30 min, and then allowed to cool. The precipitate was collected, washed with water (100 mL × 2) and purified by column chromatography using chloroform and hexane (1:1) as eluant (534 mg, 60%). ^{1}H NMR (DMSO-d_6 + $CDCl_3$, 200 MHz): δ 8.34 (m, 4H), 8.09 (m, 1H), 7.76 (m, 1H), 7.32 (m, 1H); EIMS: m/z 274 (M^+).

The above obtained compound (500 mg, 1.82 mmol) and $SnCl_2{\cdot}2H_2O$ (1.65 g, 7.3 mmol) were taken in methanol (25 mL) and refluxed for about 5 h. After completion of the reaction, the reaction mixture was concentrated and the resulting compound was suspended in 10% $NaHCO_3$ solution (100 mL), extracted with ethyl acetate (2 × 50 mL). The organic layer was concentrated under reduced pressure and purified by column chromatography using ethyl acetate and hexane (1:4) to afford compound **8a** (356 mg, 90%). ^{1}H NMR (DMSO-d_6 + $CDCl_3$, 200 MHz): δ 7.85–7.72 (m, 3H), 7.48–7.57 (m, 1H), 7.08–7.16 (m, 1H), 6.67 (d, 2H, J = 8.8 Hz), 5.08 (br s, 2H); EIMS: m/z 244 (M^+).

5.2.14. *N*1-[4-(6-Fluoro-1,3-benzothiazol-2-yl)phenyl]-5-bromopentanamide (9a)

To a mixture of **8a** (244 mg, 1.1 mmol) and triethyl amine (0.23 mL, 1.65 mmol) in THF (10 mL) at 0 °C, was added 5-bromopentanoyl chloride (300 mg, 1.65 mmol) in THF (10 mL) and the mixture was stirred at room temperature for 1 h. After completion of the reaction, the reaction mixture was concentrated and suspended in water (100 mL). The resulting precipitate was extracted with ethyl acetate (25 × 2 mL) and washed with 2 N HCl (25 mL), followed by brine. Finally, this compound was purified by column chromatography using ethyl acetate and hexane (1:4) as eluant affords compound **9a** as a pale yellow solid (300 mg, 1.5 mmol) (386 mg, yield 95%).

^{1}H NMR ($CDCl_3$ + DMSO-d_6, 200 MHz): δ 9.39 (s, 1H), 7.74–7.85 (m, 3H), 7.58–7.64 (m, 2H), 7.39–7.44 (m, 1H), 7.01–7.11 (m, 1H), 3.26–3.32 (m, 2H), 2.25–2.32 (m, 2H), 1.68–1.85 (m, 4H); LCMS: m/z 407 (M^++1), 409 (M^++3).

5.2.15. *N*1-4-Nitrobenzamide (6b)

The compound **6b** was prepared according to the method described for **6a** by employing aniline (250 mg, 1.1 mmol) and 4-nitrobenylchloride (329 mg, 1.65 mmol) affords compound **6b** as a pale yellow coloured solid (229 mg, yield 95%). ^{1}H NMR ($CDCl_3$, 300 MHz): δ 8.33 (d, 2H, J = 8.6 Hz), 8.09 (d, 2H, J = 8.6 Hz), 7.66 (m, 3H, J = 4.7 Hz), 7.07 (t, 2H, J = 8.6 Hz); EIMS: m/z 242 (M^+).

5.2.16. 4-(1,3-Benzothiazol-2-yl)aniline (8b)

The compound **8b** was prepared according to the method described for **8a** by employing **6b** (250 mg, 1.1 mmol) affords compound **8b** as a pale yellow colour solid (214 mg, yield 95%).

^{1}H NMR ($CDCl_3$, 300 MHz): δ 8.00 (d, 1H, J = 7.1), 7.92 (d, 2H, J = 8.6 Hz,), 7.81 (d, 1H, J = 7.6 Hz), 7.44 (dt, 1H, J = 7.6, 1.3 Hz), 7.34 (dt, 1H, J = 7.5, 1.2 Hz), 6.71 (d, 2H, J = 8.6 Hz), 4.04 (br s, 2H, NH_2); EIMS: m/z 226 (M^+).

5.2.17. *N*1-[4-(1,3-Benzothiazol-2-yl)phenyl]-5-bromopentanamide (9b)

The compound **9b** was prepared according to the method described for **9a** by employing **8b** (250 mg, 1.1 mmol) and 5-bromopentanoyl chloride (329 mg, 1.65 mmol) affords compound **9b** as a pale yellow coloured solid (371 mg, yield 95%). ^{1}H NMR ($CDCl_3$, 300 MHz): δ 8.00–8.10 (m, 3H), 7.88 (d, 1H, J = 8.3 Hz), 7.65 (d, 2H, J = 8.3 Hz), 7.45 (dt, 1H, J = 1.5, 8.3 Hz), 7.35 (dt, 1H, J = 1.5, 8.3 Hz), 3.45 (t, 2H, J = 6.0 Hz), 2.45 (t, 2H, J = 6.8 Hz), 2.0 (m, 4H); LCMS: m/z 389 (M^++1), 391 (M^++3).

5.2.18. *N*1-[4-(1,3-Benzothiazol-2-yl)phenyl]-4-bromobutanamide (9c)

The compound **9c** was prepared according to the method described for **9a** by employing **8b** (250 mg, 1.1 mmol) and 4-bromobutanoyl chloride (309 mg, 1.65 mmol) affords compound **9c** as a pale yellow colour solid (358 mg, yield 95%).

^{1}H NMR ($CDCl_3$, 300 MHz): δ 9.25 (br s, 1H), 7.92–8.00 (m, 3H), 7.82 (d, 1H, J = 8.6 Hz), 7.72 (d, 2H, J = 8.6 Hz), 7.40 (dt, 1H, J = 8.6, 1.6 Hz), 7.32 (dt, 1H, J = 8.6, 1.6 Hz), 3.48 (t, 2H, J = 6.3 Hz), 2.54 (t, 2H, J = 7.0 Hz), 2.18–2.24 (m, 2H); LCMS: m/z 375 (M^++1), 377 (M^++3).

5.2.19. 7-methoxy-8-{4-[4-(1,3-benzothiazol-2-yl)phenoxy]-butyl}oxy-(11a*S*)1,2,3,11a-tetra-hydro-5*H*-pyrrolo[2,1-*c*][1,4]-benzodiazepin-5-one (17a)

To a solution of **16** (246 mg, 1 mmol) in acetone (10 mL) was added K_2CO_3 (200 mg, 1.5 mmol) at 0 °C and stirred for 30 min 2-[4-(4-bromobutyloxy)-phenyl]-1,3-benzothiazole (**5a**) (433 mg, 1.20 mmol, generated freshly in acetone (10 mL) and KI (160 mg, 1 mmol), was added to the solution dropwise. The resulting solution was stirred at room temperature for 24 h. The reaction mixture was poured into ice-water (30 mL) and extracted with ethyl acetate. The combined organic phases were washed with H_2O and brine dried over Na_2SO_4 and concentrated under vacuum. The residue was subjected to column chromatography ($CHCl_3$/MeOH = 24:1) to give product as a white coloured solid (yield 295 mg, 56%). Mp 90–91 °C. $[\alpha]_D$ +154.00 (*c* 0.5, $CHCl_3$). ^{1}H NMR ($CDCl_3$, 300 MHz): δ 8.04 (d, 2H, J = 8.8 Hz), 7.90 (d, 1H, J = 8 Hz)), 7.65 (d, 1H, J = 4.0 Hz), 7.50 (s, 1H), 7.30–7.47 (m, 3H), 6.98 (d, 2H, J = 8.8 Hz), 6.82 (s, 1H), 4.05–4.21 (m, 4H), 3.94 (s, 3H), 3.50–3.85 (m, 3H), 1.90–2.30 (m, 8H); ^{13}C NMR (75 MHz, $CDCl_3$): δ 167.7, 164.6, 162.3, 161.2, 154.0, 150.8, 147.7, 140.3, 134.7, 129.0, 126.0, 124.6, 122.6, 121.3, 120.0, 114.6, 111.5, 110.1, 68.5, 67.3, 56.0, 53.8, 53.6, 46.6, 29.5, 25.9, 25.6, 24.0: FABMS: m/z 528 (M^++1). Anal. Calcd for $C_{30}H_{29}N_3O_4S$: C, 68.29; H, 5.54; N, 7.96. Found: C, 68.12; H, 5.42; N, 7.85.

5.2.20. 7-methoxy-8-{4-[4-(1,3-benzothiazol-2-yl)-2-methoxyphenoxy]butyl}oxy-(11a*S*)1,2,3,11a-tetra-hydro-5*H*-pyrrolo[2,1-*c*][1,4]benzodiazepin-5-one (17b)

The compound **17b** was prepared according to the method described for the compound **17a** by employing compound **5b** (460 mg, 1.2 mmol) as a white coloured solid (yield 334 mg, 56%). Mp 95–96 °C. $[\alpha]_D$ +159.00 (*c*, 0.5, $CHCl_3$). ^{1}H NMR ($CDCl_3$, 300 MHz): δ 8.05 (d, 1H, J = 7.8 Hz), 7.90 (d, 1H, J = 7.8 Hz), 7.64–7.72 (m, 2H), 7.30–7.62 (m, 4H), 6.96 (d, 1H, J = 7.8 Hz), 6.82 (s, 1H), 4.12–4.25 (m, 4H), 4.00 (s, 3H), 3.94 (s, 3H), 3.50–3.85 (m, 3H), 1.94–2.32 (m, 8H); ^{13}C NMR (75 MHz, $CDCl_3$): δ 167.8, 164.6, 162.3, 154.2, 150.8, 149.6, 147.7, 140.3, 134.8126.7, 126.1, 124.8, 122.7, 121.4, 121.0, 120.1, 115.5, 112.5, 110.6, 110.1, 68.5, 67.3, 56.0, 56.1, 53.8, 53.6, 46.7, 29.5, 25.9, 25.6, 24.0; FABMS: m/z 558 (M^++1). Anal. Calcd for $C_{31}H_{31}N_3O_5S$: C, 66.77; H, 5.60; N, 7.54. Found: C, 66.75; H, 5.58; N, 7.55.

5.2.21. 7-methoxy-8-{5-[4-(1,3-benzothiazol-2-yl)phenoxy] pentyl}oxy-(11a*S* 1,2,3,11a-tetra-hydro-5*H*-pyrrolo[2,1-*c*][1,4] benzodiazepin-5-one (17c)

The compound **17c** was prepared according to the method described for the compound **17a** by employing compound **5c** (450 mg, 1.2 mmol) as a white coloured solid (yield 323 mg, 60%). Mp 95–96 °C. $[\alpha]_D$ +149.00 (*c* 0.5, $CHCl_3$). ^1H NMR ($CDCl_3$, 300 MHz): δ 8.05 (d, 1H, *J* = 8.6 Hz), 7.85 (d, 1H, *J* = 8.6 Hz), 7.65 (d, 1H, *J* = 3.9 Hz), 7.30–7.55 (m, 5H), 7.0 (d, 2H, *J* = 8.6 Hz), 6.82 (s, 1H), 4.04–4.20 (m, 4H), 3.95 (s, 3H), 3.55–3.85 (m, 3H), 2.19–2.38 (m, 2H), 1.80–2.10 (m, 5H), 1.62–1.80 (m, 3H); ^{13}C NMR (75 MHz, $CDCl_3$): δ 167.7, 164.6, 162.3, 161.2, 154.0, 150.8, 147.7, 140.3, 134.7, 129.0, 126.0, 124.6, 122.6, 121.3, 120.0, 114.6, 111.5, 110.1, 68.7, 67.6, 56.0, 53.5, 46.5, 29.5, 28.8, 28.4, 23.9, 22.3; FABMS: *m/z* 542 (M^++1). Anal. Calcd for $C_{31}H_{31}N_3O_4S$: C, 68.74; H, 5.77; N, 7.76. Found: C, 68.70; H, 5.73; N, 7.74.

5.2.22. 7-methoxy-8-{5-[4-(1,3-benzothiazol-2-yl)-2-methoxy-phenoxy]pentyl}oxy-(11a*S*)1,2,3,11a-tetra-hydro-5*H*-pyrrolo-[2,1-*c*][1,4]benzodiazepin-5-one (17d)

The compound **17d** was prepared according to the method described for the compound **17a** by employing compound **5d** (486 mg, 1.2 mmol) as a white coloured solid (yield 314 mg, 55%). Mp 101–102 °C. $[\alpha]_D$ +163.00 (*c* 0.5, $CHCl_3$). ^1H NMR ($CDCl_3$, 300 MHz): δ 8.05 (d, 1H, *J* = 8.2 Hz), 7.90 (d, 1H, *J* = 8.2 Hz), 7.64–7.72 (m, 2H), 7.30–7.60 (m, 4H), 6.95 (d, 1H, *J* = 8.2 Hz), 6.80 (s, 1H), 4.06–4.18 (m, 4H), 4.00 (s, 3H), 3.95 (s, 3H), 3.50–3.80 (m, 3H), 1.62–2.34 (m, 10H); ^{13}C NMR (75 MHz, $CDCl_3$): δ 167.8, 164.6, 162.3, 154.2, 150.8, 149.6, 147.7, 140.3, 134.8126.7, 126.1, 124.8, 122.7, 121.4, 121.0, 120.1, 115.5, 112.5, 110.6, 110.1, 68.6, 67.6, 56.0, 53.6, 46.6, 29.4, 28.8, 28.5, 24.0, 22.5; FABMS: *m/z* 572 (M^++1). Anal. Calcd for $C_{32}H_{33}N_3O_5S$: C, 67.23; H, 5.82; N, 7.35. Found: C, 67.20; H, 5.81, N, 7.30.

5.2.23. 7-methoxy-8-{5-[4-(1,3-benzoxazol-2-yl)phenoxy] pentyl}oxy-(11a*S*)1,2,3,11a-tetra-hydro-5*H*-pyrrolo[2,1-*c*][1,4] benzodiazepin-5-one (17e)

The compound **17e** was prepared according to the method described for the compound **17a** by employing compound **5e** (414 mg, 1.2 mmol) as a white coloured solid (yield 263 mg, 50%). Mp 93–94 °C. $[\alpha]_D$ +155.00 (*c* 0.5, $CHCl_3$). ^1H NMR ($CDCl_3$, 300 MHz): δ 8.20 (d, 2H, *J* = 8.6 Hz), 7.72 (m, 1H), 7.65 (d, 1H, *J* = 3.9 Hz), 7.54–7.60 (m, 2H), 7.30–7.46 (m, 2H), 7.04 (d, 2H, *J* = 8.6 Hz), 6.80 (s, 1H), 4.02–4.24 (m, 4H), 3.90 (s, 3H), 3.50–3.84 (m, 3H), 2.24–2.36 (m, 2H), 1.60–2.16 (m, 8H); LCMS: *m/z* 526 (M^++1). Anal. Calcd for $C_{31}H_{31}N_3O_5$: C, 70.84; H, 5.94; N, 7.99. Found: C, 70.80; H, 5.89; N, 7.94.

5.2.24. 7-methoxy-8-{5-[4-(1,3-benzoxazol-2-yl)-2-methoxy-phenoxy]pentyl}oxy-(11a*S*)1,2,3,11a-tetra-hydro-5*H*-pyrrolo-[2,1-*c*][1,4]benzodiazepin-5-one (17f)

The compound **20f** was prepared according to the method described for the compound **17a** by employing compound **5f** (468 mg, 1.2 mmol) as a white coloured solid (yield 278 mg, 50%). Mp 98–99 °C. $[\alpha]_D$ +149.00 (*c* 0.5, $CHCl_3$). ^1H NMR ($CDCl_3$, 300 MHz): δ 7.70–7.84 (m, 3H), 7.62 (d, 1H, *J* = 4.0 Hz), 7.43–7.58 (m, 2H), 7.30–7.38 (m, 2H), 6.90 (d, 1H, *J* = 8.6 Hz), 6.80 (s, 1H), 3.88–4.20 (m, 10H), 3.50–3.80 (m, 3H), 1.60–2.36 (m, 10H); LCMS: *m/z* 556 (M^++1). Anal. Calcd for $C_{32}H_{33}N_3O_6$: C, 69.17; H, 5.99; N, 7.56. Found: C, 69.15; H, 5.89, N, 7.54.

5.2.25. 7-methoxy-8-{5-[N^1-(4-(1,3-benzothiazol-2-yl)phenyl)]pentanecarboxamide}oxy-(11a*S*)1,2,3,11a-tetra-hydro-5*H*-pyrrolo[2,1-*c*][1,4]benzodiazepin-5-one (18a)

The compound **18a** was prepared according to the method described for the compound **17a** by employing compound **9b** (465 mg, 1.2 mmol) as a pale yellow coloured solid (yield 277 mg, 50%). Mp 100–101 °C. $[\alpha]_D$ +168.00 (*c* 0.5, $CHCl_3$). ^1H NMR ($CDCl_3$, 300 MHz): δ 8.80 (s, 1H), 8.05 (m, 3H), 7.90 (d, 1H, *J* = 7.9 Hz), 7.68–7.76 (m, 3H), 7.60 (s, 1H), 7.30–7.56 (m, 2H), 6.90 (s, 1H), 4.08–4.28 (m, 2H), 3.96 (s, 3H), 3.50–3.88 (m, 3H), 2.64 (m, 2H), 1.62–2.38 (m, 8H); ^{13}C NMR (75 MHz, $CDCl_3$): δ 186.0, 168.0, 164.6, 162.3, 161.1, 154.0, 151.0, 14.7.8, 140.3, 134.6, 129.8, 126.4, 126.1, 124.8, 122.7, 121.4, 121.0, 120.0, 112.3, 111.5, 110.3, 109.8, 68.7, 56.1, 53.7, 46.6, 29.5, 28.7, 24.2, 22.4, 20.7; LCMS: *m/z* 555 (M^++1). Anal. Calcd for $C_{31}H_{30}N_4O_4S$: C, 67.13; H, 5.45; N, 10.10. Found: C, 67.10; H, 5.08; N, 9.95.

5.2.26. 7-methoxy-8-{5-[N^1-(4-(6-fluoro-1,3-benzothiazol-2-yl)phenyl)]pentane carboxa-mide}oxy-(11a*S*)1,2,3,11a-tetra-hydro-5*H*-pyrrolo[2,1-*c*][1,4]benzodiazepin-5-one (18b)

The compound **17b** was prepared according to the method described for the compound **17a** by employing compound **9a** (487 mg, 1.2 mmol) as a pale yellow coloured solid (yield 286 mg, 50%). Mp 102 °C. $[\alpha]_D$ +170.00 (*c* 0.5, $CHCl_3$). ^1H NMR ($CDCl_3$, 300 MHz): δ 8.88 (br s, 1H), 7.90–8.05 (m, 4H), 7.64–7.76 (m, 3H), 7.58 (m, 1H), 7.20 (m, 1H), 6.84 (s, 1H), 4.12–4.36 (m, 2H), 3.94 (s, 3H), 3.50–3.88 (m, 3H), 2.50–2.70 (m, 2H), 1.65–2.40 (m, 8H); LCMS: *m/z* 573 (M^++1). Anal. Calcd for $C_{31}H_{29}FN_4O_4S$: C, 65.02; H, 5.10; N, 9.78. Found: C, 65.00; H, 5.08; N, 9.73.

5.2.27. *N*-(4-(1,3-Benzothiazolyl)phenyl)-2-pyrrolidinone (19)

When two compounds **9c** (375 mg, 1 mmol) and **16** (400 mg, 1 mmol) were reacted together according to the method described for **17a**, the expected **18c** was not obtained, instead **9c** was cyclized to the compound **19** (yield 205 mg, 70%). ^1H NMR ($CDCl_3$, 300 MHz): δ 8.10 (td, 2H, *J* = 2.26, 8.3 Hz), 8.05 (d, 1H, *J* = 8.3 Hz), 7.90 (d, 1H, *J* = 8.3 Hz), 7.80 (td, 2H, *J* = 2.26, 8.3 Hz), 7.49 (dt, 1H, *J* = 6.8, 1.5 Hz), 7.39 (dt, 1H, *J* = 6.8, 1.5 Hz), 3.95 (t, 2H, *J* = 6.8 Hz), 2.67 (t, 2H, *J* = 8.3 Hz), 2.18–2.30 (m, 2H); ESIMS: *m/z* 295 (M^++1).

5.3. Anticancer activity

The compounds **17a–d** and **18a** were evaluated for in vitro activity against selected human tumour cell lines, derived from six cancer types (lung cancer, cervix cancer, breast cancer, prostate cancer, colon cancer and ovarian cancer). For each compound, dose–response curves against each cell line were measured. Sulforhodamine B (SRB) protein assay has been used to estimate cell viability or growth.

5.4. Thermal denaturation studies

Compounds were subjected to thermal denaturation studies with duplex-form CT-DNA using reported method. Working solutions in aqueous buffer (10 mM NaH_2PO_4/Na_2HPO_4, 1 mM Na_2EDTA, pH 7.00 + 0.01) containing CT-DNA (100 μM in phosphate) and the PBD (20 μM) were prepared by addition of concentrated PBD solutions in DMSO to obtain a fixed [PBD]/[DNA] molar ratio of 1:5. The DNA–PBD solutions were incubated at 37 °C for 0, 18 and 36 h prior to analysis. Samples were monitored at 260 nm using a Beckman–Coulter DU 800 spectrophotometer fitted with high performance temperature controller, and heating was applied at 1 °C min^{-1} in the range of 40–90 °C. DNA helix→coil transition temperatures *I* were obtained from the maxima in the $d(A_{260})/dT$ derivative plots. Results are given as means ± standard deviation from three determinations and are corrected for the effects of DMSO co-solvent using a linear correction term. Drug-induced alterations in DNA melting behaviour are given by $\Delta T_m = T_m$ (DNA + PBD) − T_m(DNA alone), where the T_m value for the PBD-free CT-DNA is 69.2 ± 0.01 °C. The fixed [PBD]/[DNA] ratio used did not

result in binding saturation of the host DNA duplex for any compound examined.

5.5. Restriction endonuclease inhibition

Stock solutions of each PBD (100 μM) were prepared by dissolving each compound in DMSO (Sigma). These were stored at −20 °C. Plasmid (pBR 322) containing single *BamHI* site was used in this assay. Restriction endonuclease and the relevant buffer were obtained from NEB. The DNA fragment (500 ng) was incubated with each PBD (see Fig. 2 for PBD concentrations) in a final volume of 16 μL for 16 h at 37 °C. Next 10× *BamHI* buffer (2 μL) was added, and the reaction mixture was made up to 20 μL with *BamHI* (20 U) and then incubated for 1 h at 37 °C. Then loaded on to a 1% agarose gel electrophoresis in Tris–acetate EDTA buffer at 80 V for 2 h. The gels were stained with ethidium bromide and photographed.

5.6. Molecular modelling

5.6.1. Docking

The GOLD 3.2 program protocol[20] was used for the molecular docking calculations of the cross-linked complex formed between the synthesized molecules and the host DNA duplex. All molecules were prepared using SYBYL6.9 (Tripos Inc., St. Louis, MO). Tripos force field and Gasteiger–Hückel partial atomic charges were applied with distance dependent dielectric constant and Powell's conjugate gradient energy minimization method with a convergence criterion of 0.001 kcal/mol was reached. The B-DNA duplex was built and minimized using 'nucgen' and 'sander' modules of AMBER, suit of programs, respectively. The parameter set for docking was as follows: number of islands 5, population size of 100, number of operations was 100,000, a niche size of 2 and a selection pressure of 1.1 and the van der Waals and hydrogen bonding were set to 4.0 and 2.5, respectively.

5.6.2. Molecular dynamics simulations

Ligand parameters and charges were determined with the antechamber module of AMBER 8 based on the general atom force field (GAFF)[25] and the AM1-BCC charge scheme.[26,27] Since for most of the ligands complete GAFF parameter set could not be generated, we used an alternative, second parametrization in which parameters for bonds, valence, dihedral and improper angles were adjusted using the prmchk command of AMBER.[28]

The complex is solvated with TIP3P water in the 10 Å periodic box. Equilibration of the solvated complex has been done by carrying out a minimization (500 steps of each steepest descent and conjugate gradient method), 50 ps of heating and 50 ps of density equilibration with weak restraints on the complex followed by 500 ps of constant pressure equilibration at 300 K. Twelve angstroms cut off distance for the long range non-bonded interactions is used. Shake method is applied on hydrogen atoms, a 2 fs time step and Langevin dynamics for temperature control. The same conditions as the final phase of equilibration are used for production run. The final production run is performed for the 2 ns and the coordinates are recorded in every 10 ps.

5.6.3. MM-PBSA calculations

Solute configurations DNA, ligand and complex (without water) are sampled from the final MD trajectory. The energy terms are averaged over 200 frames extracted from MD simulation trajectories, in the standard MM-PB(GB)SA protocol. For each solute configuration, the gas-phase energy is estimated using the same molecular mechanics potential that was used to perform the simulation, but all solvent molecules are ignored, and no cutoffs are used in evaluating the non-bonded interactions. Free energies of solvation are then reintroduced by using a numerical Poisson−Boltzmann calculation for the electrostatic portion and a surface-area-dependent term for non-electrostatic contributions to salvation.[21]

5.7. Cell cycle analysis

5×10^5 each of A375 cells were seeded in 60 mm dish and were allowed to grow for 24 h. Compounds **17b**, **17d**, **18a** and DC-81 were added at a final concentration 2 μM to the culture media, and the cells were incubated for an additional 24 h. Harvesting of cells was done with trypsin–EDTA, and fixed with ice-cold 70% ethanol at 4 °C for 30 min, washed with PBS and incubated with 1 mg/mL Rnase A solution at 37 °C for 30 min. Cells were collected by centrifugation at 2000 rpm for 5 min and were stained with propidium iodide (PI) [10 mg of propidium iodide (PI), 0.1 mg of trisodium citrate and 0.03 mL of Triton X-100 were dissolved in 100 mL of sterile MilliQ water at room temperature for 30 min in the dark]. The DNA contents of 20,000 events were measured by flow cytometer (DAKO CYTOMATION, Beckman Coulter, Brea, CA). Histograms were analyzed using Summit Software.

Acknowledgements

The authors K.S.R, M.N.A.K. and R.V.C.R.N.C.S. thank CSIR and the Department of Biotechnology, New Delhi (BT/PR/7037/Med/14/933/2006); for financial assistance.

References and notes

1. (a) Thurston, D. E.; Bose, D. S. *Chem. Rev.* **1994**, *94*, 433; (b) Kamal, A.; Azeeza, S.; Bharathi, E. V.; Malik, M. S.; Shetti, R. V. C. R. N. C. *Mini.-Rev. Med. Chem.*, in press.
2. Petrusek, R. L.; Uhlenhopp, E. L.; Duteau, N.; Hurley, L. H. *J. Biol. Chem.* **1982**, *257*, 6207.
3. (a) Dervan, P. B. *Science* **1986**, *232*, 464; (b) Hurley, L. H.; Boyd, F. L. *TIPS* **1988**, *9*, 402; (c) Hurley, L. H. *J. Med. Chem.* **1989**, *32*, 2027.
4. (a) Antonow, D.; Kaliszczak, M.; Kang, G.-D.; Coffils, M.; Tiberghien, A. C.; Cooper, N.; Barata, T.; Heidelberger, S.; James, C. H.; Zloh, M.; Jenkins, T. C.; Reszka, A. P.; Neidle, S.; Guichard, S. M.; Jodrell, D. I.; Hartley, J. A.; Howard, P. W.; Thurston, D. E. *J. Med. Chem.* **2010**, *53*, 2927; (b) Rahman, K. M.; Thompson, A. S.; James, C. H.; Narayanaswamy, M.; Thurston, D. E. *J. Am. Chem. Soc.* **2009**, *131*, 1375; (c) Rettig, M.; Weingarth, M.; Langel, W.; Kamal, A.; Kumar, P. P.; Weisz, K. *Biochemistry* **2009**, *48*, 12223; (d) Kamal, A.; Rao, M. V.; Laxman, N.; Ramesh, G.; Reddy, G. S. K. *Curr. Med. Chem. Anticancer Agents* **2002**, *2*, 215; (e) Kamal, A.; Ramesh, G.; Laxman, N.; Ramulu, P.; Srinivas, O.; Neelima, K.; Kondapi, A. K.; Srinu, V. B.; Nagarajaram, H. A. *J. Med. Chem.* **2002**, *45*, 4679; (f) Wells, G.; Martin, C. R. H.; Howard, P. W.; Sands, Z. A.; Laughton, C. A.; Tiberghien, A.; Woo, C. K.; Masterson, L. A.; Stephenson, M. J.; Hartley, J. A.; Jenkins, T. C.; Shnyder, S. D.; Loadman, P. M.; Waring, M. J.; Thurston, D. E. *J. Med. Chem.* **2006**, *49*, 5442; (g) Hu, W.-P.; Ling, J.-J.; Kao, C.-L.; Chen, Y.-C.; Chen, C.-Y.; Tsai, F.-Y.; Wu, M.-J.; Chang, L.-S.; Wang, J.-J. *Bioorg. Med. Chem.* **2009**, *17*, 1172.
5. Alley, M. C.; Hollingshead, M. G.; Pacula-Cox, C. M.; Waud, W. R.; Hartley, J. A.; Howard, P. W.; Gregson, S. J.; Thurston, D. E.; Sausville, E. A. *Cancer Res.* **2004**, *64*, 6693.
6. (a) Caleta, I.; Kralj, M.; Branimir Bertosa, B.; Sanja Tomic, S.; Pavlovic, G.; Pavelic, K.; Karminski-Zamola, G. *J. Med. Chem.* **2009**, *52*, 1744; (b) Chung, Y.; Shin, Y.-K.; Zhan, C.-G.; Lee, S.; Cho, H. *Arch. Pharmacol. Res.* **2004**, *27*, 893; (c) Yoshida, M.; Hayakawa, I.; Hayashi, N.; Agatsuma, T.; Oda, Y.; Tanzawa, F.; Iwasaki, S.; Koyama, K.; Furukawa, H.; Kurakata, S. *Bioorg. Med. Chem. Lett.* **2005**, *15*, 3328.
7. (a) Bradshaw, T. D.; Stevens, M. F. G.; Westwell, A. D. *Curr. Med. Chem.* **2001**, *8*, 203; (b) Hutchinson, I.; Chua, M.-S.; Browne, H. L.; Trapani, V.; Bradshaw, T. D.; Westwell, A. D.; Stevens, M. F. G. *J. Med. Chem.* **2001**, *44*, 1446.
8. (a) Chua, M.-S.; Shi, D.-F.; Wrigley, S.; Bradshaw, T. D.; Hutchinson, I.; Shaw, P. N.; Barrett, D. A.; Stanley, L. A.; Stevens, M. F. G. *J. Med. Chem.* **1999**, *42*, 381; (b) Kashiyama, E.; Hutchinson, I.; Chua, M.-S.; Stinson, S. F.; Phillips, L. R.; Kaur, G.; Sausville, E. A.; Bradshaw, T. D.; Westwell, A. D.; Stevens, M. F. G. *J. Med. Chem.* **1999**, *42*, 4172.
9. O'Brien, S. E.; Browne, H. L.; Bradshaw, T. D.; Westwell, A. D.; Stevens, M. F. G.; Laughton, C. A. *Org. Biomol. Chem.* **2003**, *1*, 493.
10. Mortimer, C. G.; Wells, G.; Crochard, J.-P.; Stone, E. L.; Bradshaw, T. D.; Stevens, M. F. G.; Westwell, A. D. *J. Med. Chem.* **2006**, *49*, 179.
11. (a) Kumar, D.; Jacob, M. R.; Reynolds, M. B.; Kerwin, S. M. *Bioorg. Med. Chem.* **2002**, *10*, 3997; (b) Huagn, S. T.; Hsei, I.-J.; Chen, C. *Bioorg. Med. Chem.* **2006**, *14*, 6106.

12. (a) Kamal, A.; Khan, M. N. A.; Srikanth, Y. V. V.; Reddy, K. S.; Juvekar, A.; Sen, S.; Kurian, N.; Zingde, S. *Bioorg. Med. Chem.* **2008**, *16*, 7804; (b) Kamal, A.; Khan, M. N. A.; Reddy, K. S.; Ahmed, S. K.; Kumar, M. S.; Juvekar, A.; Sen, S.; Zingde, S. *Bioorg. Med. Chem. Lett.* **2007**, *17*, 5345; (c) Kamal, A.; Ramulu, P.; Srinivas, O.; Ramesh, G. *Bioorg. Med. Chem. Lett.* **2003**, *13*, 3517; (d) Kamal, A.; Srinivas, O.; Ramulu, P.; Ramesh, G.; Kumar, P. P. *Bioorg. Med. Chem. Lett.* **2004**, *14*, 4107; (e) Kamal, A.; Reddy, P. S. M. M.; Reddy, D. R.; Laxman, E. *Bioorg. Med. Chem.* **2006**, *14*, 385; (f) Kamal, A.; Bharathi, E. V.; Ramaiah, M. J.; Dastagiri, D.; Reddy, J. S.; Vishwanath, V.; Sulthana, F.; Pushpavalli, S. N. C. V. L.; Bhadra, M.-P.; Srivastava, H. K.; Sastry, G. N.; Juvekar, A.; Sen, S.; Zingde, S. *Bioorg. Med. Chem.* **2010**, *18*, 526; (g) Kamal, A.; Sreekanth, K.; Kumar, P.; Shankaraiah, N.; Balakishan, G.; Ramaiah, M. J.; Pushpavalli, S. N. C. V. L.; Ray, P.; Bhadra, M.-P. *Eur. J. Med. Chem.* **2010**, *45*, 2173; (h) Kamal, A.; Rajender; Reddy, D. R.; Reddy, M. K.; Balakishan, G.; Shaik, T. B.; Chourasia, M.; Sastry, G. N. *Bioorg. Med. Chem.* **2009**, *17*, 1557.
13. Centore, R.; Panunzi, B.; Roviello, A.; Villano, P. *J. Polym. Sci., Part A: Polym. Chem.* **1996**, *34*, 3203.
14. Karlsson, J.; Bergqvist, M. H.; Lincoln, P.; Westman, G. *Bioorg. Med. Chem.* **2004**, *12*, 2369.
15. Thurston, D. E.; Murty, V. S.; Langley, D. R.; Jones, G. B. *Synthesis* **1990**, 81.
16. Sedlak, M.; Hejtmankova, L.; Kasparova, P.; Kavalek, J. *J. Phys. Org. Chem.* **2002**, *15*, 165.
17. Jones, G. B.; Davey, C. L.; Jenkins, T. C.; Kamal, A.; Kneale, G. G.; Neidle, S.; Webster, G. D.; Thurston, D. E. *Anti-Cancer Drug Des.* **1990**, *5*, 249.
18. Puvvada, M. S.; Hartley, J. A.; Jenkins, T. C.; Thurston, D. E. *Nucleic Acids Res.* **1993**, *21*, 3671.
19. (a) Srivani, P.; Sastry, G. N. *J. Mol. Graphics Modell.* **2009**, *27*, 676; (b) Srivani, P.; Srinivas, E.; Raghu, R.; Sastry, G. N. *J. Mol. Graphics Modell.* **2007**, *26*, 378; (c) Ravindra, G. K.; Achaiah, G.; Sastry, G. N. *Eur. J. Med. Chem.* **2008**, *43*, 830.
20. Ryckaert, J. P.; Ciccotti, G.; Berendsen, H. J. C. *J. Comput. Phys.* **1977**, *23*, 327.
21. Wilson, W. D.; Nguyen, B.; Tanious, F. A.; Mathis, A.; Hall, J. E.; Stephens, C. E.; Boykin, D. W. *Curr. Med. Chem. Anticancer Agents* **2005**, *5*, 389.
22. Neidle, S. *Nat. Prod. Rep.* **2001**, *18*, 291.
23. Kollman, P. A.; Massova, I.; Reyes, C.; Kuhn, B.; Huo, S.; Chong, L.; Lee, M.; Lee, T.; Duan, Y.; Wang, W.; Donini, O.; Cieplak, P.; Srinivasan, J.; Case, D. A.; Cheatham, T. E., III *Acc. Chem. Res.* **2000**, *33*, 889.
24. Skehan, P.; Storeng, R.; Scudiero, D.; Monks, A.; McMahon, J.; Vistica, D.; Warren, J. T.; Bokesch, H.; Kenney, S.; Boyd, M. R. *J. Natl. Cancer Inst.* **1990**, *82*, 1107.
25. Wang, J.; Wolf, R. M.; Caldwell, J. W.; Kollman, P. A.; Case, D. A. *J. Comput. Chem.* **2004**, *25*, 1157.
26. Jakalian, A.; Bush, B. L.; Jack, D. B.; Bayly, C. I. *J. Comput. Chem.* **2000**, *21*, 132.
27. Jakalian, A.; Jack, D. B.; Bayly, C. I. *J. Comput. Chem.* **2002**, *23*, 1623.
28. Gerber, P. R.; Mueller, K. *J. Comput. Aided Mol. Des.* **1995**, *9*, 251.